22. Monastirioti M, Giagtzoglou N, Koumbanakis K, et al. Drosophila Hey is a target of Notch in asymmetric divisions during embryonic and larval neurogenesis. *Development*. 2010;137:191–201.
23. Mukhopadhyay A, Jarrett J, Chlon T, et al. HeyL regulates the number of TrkC neurons in dorsal root ganglia. *Dev Biol*. 2009;334:142–151.
24. Chen H, Thiagalingam A, Chopra H, et al. Conservation of the Drosophila lateral inhibition pathway in human lung cancer: a hairy-related protein (HES-1) directly represses achaete-scute homolog-1 expression. *Proc Natl Acad Sci U S A*. 1997;94:5355–5360.
25. Gersemann M, Becker S, Kubler I, et al. Differences in goblet cell differentiation between Crohn's disease and ulcerative colitis. *Differentiation*. 2009;77:84–94.
26. Shroyer NF, Helmrath MA, Wang VYC, et al. Intestine-specific ablation of mouse atonal homolog 1 (Math1) reveals a role in cellular homeostasis. *Gastroenterology*. 2007;132:2478–2488.
27. Dahan S, Roda G, Pinn D, et al. Epithelial: lamina propria lymphocyte interactions promote epithelial cell differentiation. *Gastroenterology*. 2008;134:192–203.
28. Colleypriest B, Palmer R, Ward S, et al. Cdx genes, inflammation and the pathogenesis of Barrett's metaplasia. *Trends Mol Med*. 2009;15: 313–322.
29. Eda A, Osawa H, Yanaka I, et al. Expression of homeobox gene CDX2 precedes that of CDX1 during the progression of intestinal metaplasia. *J Gastroenterol*. 2002;37:94–100.
30. Zheng J, Sun X, Wang W, et al. Hypoxia-inducible factor-1alpha modulates the down-regulation of the homeodomain protein CDX2 in colorectal cancer. *Oncol Rep*. 2010;24:97–104.
31. Giatromanolaki A, Sivridis E, Maltezos E, et al. Hypoxia inducible factor 1alpha and 2alpha overexpression in inflammatory bowel disease. *J Clin Pathol*. 2003;56:209–213.

J Gastroenterol (2011) 46:191–202
DOI 10.1007/s00535-010-0346-x

ORIGINAL ARTICLE—ALIMENTARY TRACT

Longitudinal cell formation in the entire human small intestine is correlated with the localization of Hath1 and Klf4

Michiko Iwasaki · Kiichiro Tsuchiya · Ryuichi Okamoto · Xiu Zheng · Yoshihito Kano · Eiko Okamoto · Eriko Okada · Akihiro Araki · Shinji Suzuki · Naoya Sakamoto · Keisuke Kitagaki · Takumi Akashi · Yoshinobu Eishi · Tetsuya Nakamura · Mamoru Watanabe

Received: 26 July 2010 / Accepted: 18 October 2010 / Published online: 3 December 2010

Abstract
Background Double balloon endoscopy (DBE) enables the observation and collection of viable specimens from the entire intestine, thereby allowing more detailed investigation of how the structure and function of the human small intestine are regulated. The present study aimed to elucidate the regulation of cell formation in the human small intestine using biopsy specimens collected from an entire individual small intestine by DBE.

Methods The expression and the localization of representative genes for the differentiation program were analyzed in the entire small intestine of 10 patients. The functional correlation between Hath1 and Klf4 was analyzed in an intestinal cell line by using a Tet-On system.

Results In longitudinal cell formation in the small intestine, it was shown that goblet cells, but not Paneth cells, increased toward the ileum in each individual small intestine. Immunohistochemistry showed that Hath1-expressing cells migrated from the base of the crypt to the top of the villi in the terminal ileum, while Klf4-expressing cells migrated from the top of the villus, resulting in the colocalization of Hath1 and Klf4 in the terminal ileum. Coexpression of Hath1 and Klf4 upregulated the expression of phenotypic genes for goblet cells following the downregulation of those for Paneth cells.

Conclusions Using mapping biopsy by DBE, we have demonstrated, for the first time, the molecular basis of the villus structure in the entire human small intestine in vivo. The present study showed that longitudinal cell formation was regulated by the colocalization of Hath1 and Klf4 that converted Paneth cell differentiation into goblet cell differentiation.

Keywords Double balloon endoscopy · Goblet cells · Paneth cells · Hath1 · Atoh1

M. Iwasaki and K. Tsuchiya contributed equally to this work.

Electronic supplementary material The online version of this article (doi:10.1007/s00535-010-0346-x) contains supplementary material, which is available to authorized users.

M. Iwasaki · K. Tsuchiya · R. Okamoto · X. Zheng · Y. Kano · E. Okamoto · E. Okada · A. Araki · S. Suzuki · N. Sakamoto · T. Nakamura · M. Watanabe (✉)
Department of Gastroenterology and Hepatology, Graduate School, Tokyo Medical and Dental University, 1-5-45, Yushima, Bunkyo-ku, Tokyo 113-8519, Japan
e-mail: mamoru.gast@tmd.ac.jp

R. Okamoto · T. Nakamura
Department of Advanced Therapeutics in Gastrointestinal Diseases, Graduate School, Tokyo Medical and Dental University, Tokyo, Japan

N. Sakamoto
Department for Hepatitis Control, Tokyo Medical and Dental University, Tokyo, Japan

E. Okada · A. Araki
Department of Endoscopic Diagnosis and Therapy, Tokyo Medical and Dental University, Tokyo, Japan

K. Kitagaki · T. Akashi · Y. Eishi
Department of Pathology, Graduate School, Tokyo Medical and Dental University, Tokyo, Japan

Introduction

The six-meter length of the human small intestine consisting of the jejunum and ileum had long been considered a "dark continent" because of the lack of devices to observe its whole length easily. Recently, however, powerful tools have been developed to visualize the whole

human intestinal tract, such as capsule endoscopy (CE) [1, 2] and double balloon endoscopy (DBE) [3–5]. These have revealed an unexpectedly large number of diseases of the small intestine, such as cancers, malignant lymphomas, ulcers, and vascular lesions [6, 7]. At the same time, a number of ulcerous and erosive lesions found by histopathological examination of biopsy specimens have been observed as unknown diseases with nonspecific inflammation [8]. Therefore, elucidation of pathobiological regulation in the human small intestine is essential to resolve the difficulty of diagnosing the various lesions in the small intestine.

Despite the multiple roles of the small intestine in homeostasis, such as digestion, absorption, immune regulation, hormone secretion, peristaltic movement, and the regeneration of intestinal epithelial cells (IECs) [9–12], the overall function of the entire small intestine has never been considered. Although the horizontal structure of the small intestine has been elucidated as showing axial regulation from crypt base to villus top under the control of various signal transduction pathways, such as Wnt, Notch, and bone morphogenetic protein (BMP) [13–16], the regulation of its longitudinal structure remains to be elucidated, especially in humans. An understanding of the molecular basis of the structure of the human intestine has been thought to be indispensable for elucidating the pathology of human intestinal disease. One of the most important genes for the formation of IECs is that for the basic helix-loop-helix (bHLH) transcription factor, Atoh1, and its human homolog, Hath1, which is essential for cellular differentiation toward secretory lineages in the small and large intestine [17]. According to our recent studies, failure of the differentiation system in the human colon is caused by the deregulation of crucial genes for the construction of IECs with aberrant cell signaling induced by the pathology of intestinal diseases, such as colon cancer and ulcerative colitis [18, 19].

It has been suggested that regional functions of the small intestine might be different, with rigid regulation for the immediate situation in each region from the proximal side to the distal side. However, the regional roles of IECs have been poorly investigated, except for their part in nutritional absorption and hormone secretion [9, 20]. Moreover, it remains unknown how the ratio of the four lineages of IECs—goblet cells, enteroendocrine cells, Paneth cells, and absorptive enterocytes—is regulated to fit to regional function in the human small intestine. Hitherto, analyses of regional function in the human small intestine have employed specimens originating from operative tissues of different individuals [21, 22]. Accordingly, those results are not precisely comparable because of individual differences, although it has been widely considered that the number of goblet cells and Paneth cells increases toward the terminal ileum.

Although cellular differentiation into goblet cells is regulated by Atoh1 and a zinc-finger type transcriptional factor, Kruppel-like factor 4 (Klf4) [17, 23], the mechanism by which goblet cells increase in number toward the terminal ileum has not yet been elucidated.

In this study, we performed a mapping biopsy of the entire human small intestine using DBE to elucidate the regional regulation of cell formation in the villi. We found an increase in the number of goblet cells, but not Paneth cells, toward the terminal ileum. The colocalization of Hath1 and Klf4 proteins changed cellular differentiation to Paneth cells to differentiation to goblet cells, regulating the longitudinal differentiation of cells in the human small intestine.

Materials and methods

Human small intestinal tissue

Human tissue specimens were obtained from patients with an indication to undergo DBE at Tokyo Medical and Dental University Hospital because of obscure gastrointestinal bleeding. To analyze the structure of the normal small intestine, we selected biopsy specimens from 10 patients who showed no abnormality in the small intestine by subsequent DBE. Patients with abnormal findings in the small intestine by DBE and those who were taking medication that might injure the small intestinal mucosa were excluded. To measure villus size, tissue specimens from 20 patients with no abnormality in the small intestine by DBE were used. Written informed consent was obtained from each patient, and the experiments were approved by the Tokyo Medical and Dental University Hospital Ethics Committee for Human Subjects.

The proximal two-fifths of the small intestine was observed via the oral insertion route, and biopsy specimens were taken from two locations at approximately equal intervals. On another day, the distal three-fifths of the small intestine was observed via the anal insertion route, and biopsy specimens were taken from three locations at approximately equal intervals. Biopsy intervals were confirmed from the position of the endoscope tip visualized by X-ray and from the insertion length of the endoscope calculated by addition of the insertion lengths in each operation. Three biopsy specimens were taken from each of the five locations in each patient to generate RNA, paraffin sections, and frozen sections, respectively. Each biopsy specimen was numbered 1–5 from the proximal side.

Quantitative real-time polymerase chain reaction (PCR)

Total RNA was isolated using TRIzol reagent (Invitrogen; Carlsbad, CA, USA). Aliquots of 1 μg of total RNA were used for reverse transcription (Qiagen; Valencia, CA, USA). Quantitative PCRs were carried out using a Light-Cycler system (Roche Diagnostics; Mannheim, Germany). The primer sequences are summarized in supplementary Table S1. In the analysis of small intestine biopsy specimens, the expression of the most proximal specimen was taken as 1 in order to compensate for individual differences.

Histology and immunohistochemistry

Histological analysis of human small intestines was performed by using hematoxylin and eosin (H&E)-stained slices or periodic acid-Schiff (PAS)-stained slices generated from paraffin sections. The height and width of the villus mucosa and the depth of crypts were measured with a Micro Analyzer (Japan Poladigital; Tokyo, Japan). Three villi and crypts per slide of each region in 10 patients were measured.

Immunohistochemical findings from human small intestines were assessed by using frozen sections. Hath1 antibody was originally generated as previously described [18]. Hes1 antibody was the same as that used in a previous study [19]. The other antibodies used were anti-human chromogranin A (CgA) (DAKO; Glostrup, Denmark), anti-human Klf4 (H-180; Santa Cruz Biotechnology; Santa Cruz, CA, USA), and anti-human TFF3 (ab57752; Abcam; Cambridge, UK). The standard avidin-biotin-peroxidase (ABC) method (Vectastain; Vector Laboratories; Burlingame, CA, USA) was used, and staining was developed by the addition of diaminobenzidine (Vector Laboratories).

Goblet cells were counted per 300 epithelial cells. Paneth cells were counted per crypt. These two types of cells were counted on H&E-stained slices. Endocrine cells were counted as CgA-positive cells per 300 epithelial cells on CgA-immunostained slices. The number of absorptive cells was calculated by subtracting the goblet cell and CgA-positive cell numbers from the total number.

Cell culture

Human colon cancer-derived LS174T cells were grown in minimum essential medium (Gibco; Billings, MT, USA) supplemented with 10% fetal bovine serum and 1% penicillin–streptomycin. The cell cultures and plasmid DNA transfections were performed as previously described [24]. A cell line expressing Klf4 (Tet-On Klf4 cells) under the control of doxycycline (DOX, 100 ng/ml; Clontech; Mountain View, CA, USA) was generated as previously described [25].

Plasmids

Hath1-lentivirus vector was generated by inserting the PCR-amplified Hath1 gene into pLenti6.4 (Invitrogen). Hath1-lentivirus was generated according to the manufacturer's protocols.

Tetracycline-dependent expression of Klf4 was achieved by cloning the gene encoding the open reading frame of the human Klf4 into the pcDNA4/TO/myc-his vector (Invitrogen). All constructs were confirmed by DNA sequencing.

Statistical analyses

In the quantitative real-time PCR analysis of small-intestine biopsy specimens, groups of data were compared using the Mann–Whitney *U*-test. *P* values of less than 0.05 were considered statistically significant.

Other data were statistically analyzed with paired Student's *t*-tests. *P* values of less than 0.05 were considered statistically significant.

Results

The villus height, width, and crypt depth in an entire small intestine were the same in all longitudinal regions

While regional differences between the jejunum and the ileum have been found anatomically, distinct differences between them in villus structure have not been suggested. Moreover, the precise mechanism for the formation of a regional villus structure has not been examined in a full-length small intestine in an "alive environment". We therefore performed mapping biopsy of the full-length small intestine in 10 people who had an indication for DBE. We determined the positions for biopsy with the assistance of X-ray images and the insertion length of the endoscope in order to take five biopsy specimens at equal intervals from the ligament of Treitz to Bauhin's valve. The resulting regions were numbered 1–5 from the proximal side (Fig. 1a). The endoscopic findings of the whole small intestine were normal, and neither inflammation nor erosion was found by pathological examinations of biopsy samples (Fig. 1b).

We first analyzed the villus size, dividing it into height, width, and crypt depth, throughout the small intestine. Unexpectedly, the villus size in each of 20 people was almost the same in any region of the small intestine (Fig. 1c). Previous reports showed that the villi became

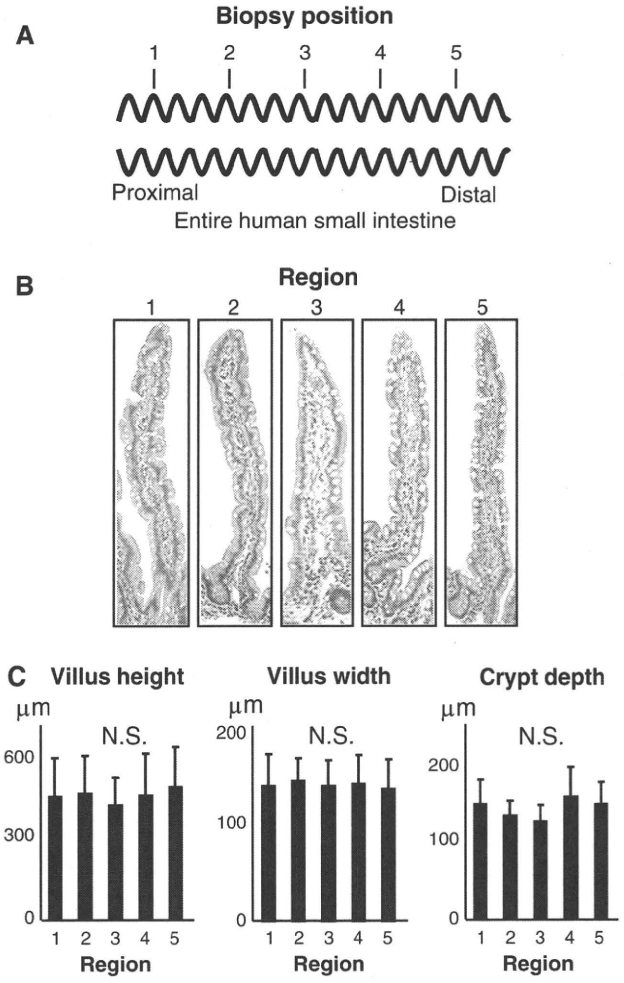

Fig. 1 Structure of villi and crypts throughout the entire human small intestine. **a** Schematic representation of the position for mapping biopsy by double balloon endoscopy (DBE). **b** H&E-stained sections of biopsy specimens (×10). Specimens are numbered 1–5 from proximal to distal regions. Fundamental structures of villi and crypts do not change throughout the entire human small intestine. Paneth cells are observed as acidophilic cells at the base of crypts. **c** Villus height, villus width, and crypt depth. The size of villi and crypts was constant from proximal to distal regions (differences not significant, $P > 0.05$, $n = 20$). *N.S.* Not significant

shorter and wider toward the terminal ileum in rats [26]. In humans, in studies using operative or anatomical tissues, it has also been thought that villus length was greater at the proximal jejunum than at the terminal ileum; however, the villus size of the entire small intestine of the same person has never been analyzed in vivo.

Goblet cells increased toward the terminal ileum, while Paneth cells were maintained

We next assessed the longitudinal change of cell formation in the villi of individual human small intestines by counting each of four types of IECs in each region. PAS staining showed a phased increase of goblet cells toward the terminal ileum (Fig. 2a, d), while surprisingly, the number of Paneth cells per crypt was unchanged, which contradicts the widely accepted hypothesis that Paneth cells are increased toward the terminal ileum (Fig. 2b, d). CgA-positive cells were counted as endocrine cells (Fig. 2c, d), and cells other than the foregoing three types were counted as absorptive cells, and their numbers decreased toward the terminal ileum (Fig. 2d).

We also assessed the regional expression of representative genes for each type of cell to confirm whether gene expression parallels cell formation in each region of the small intestine. Quantitative real-time PCR revealed considerable individual differences between the 10 people in gene expression at the same position in the small intestine (Fig. 2e). To compensate for this, the gene expression in each region was expressed relative to that in region 1 in the jejunum, which was taken as unity. MUC2 gene expression gradually increased in the same way as the cell formation. In regions 4 and 5, MUC2 expression was significantly increased compared with that in region 1, while lactase gene expression was significantly decreased compared with that in region 1.

Interestingly, the expression of HD5 was almost constant throughout the small intestine, consistent with Paneth cell formation, and differed from expectations that antimicrobial peptides would be induced by the increase of enterobacteria in the terminal ileum. The quantities of intestinal epithelial cells included in each biopsy specimen were found to be constant by cytokeratin 19 (CK19) quantification in each region (Supplemental Fig. 1).

The increase of Hath1 gene expression at the terminal ileum is independent of the Notch signal

To clarify how the transition of cell formation in each region is regulated, we examined the gene expression of Hath1 and Hes1, because the Notch signal determines the fate of IECs, especially the differences between absorptive cells and secretory cells, through the expression of the Hes1 and Hath1 genes, respectively, as we and others have previously described [14, 19]. The Hath1 genes were upregulated toward the terminal ileum, while Hes1 gene expression was unchanged (Fig. 3a). We also analyzed the localization of Hath1 in the villi in each region. In region 1, Hath1-positive cells were found only at the crypt base. However, toward the ileum, Hath1 expression gradually ascended to the villi. Finally, in region 5, Hath1-positive cells were found throughout the whole villus (Fig. 3b). In contrast, Hes1-positive cells were found in the crypt base in all regions of the human small intestine (Fig. 3b). We also counted the number of each type of protein-positive cell in each region. In the crypts, Hath1- and Hes1-positive cells

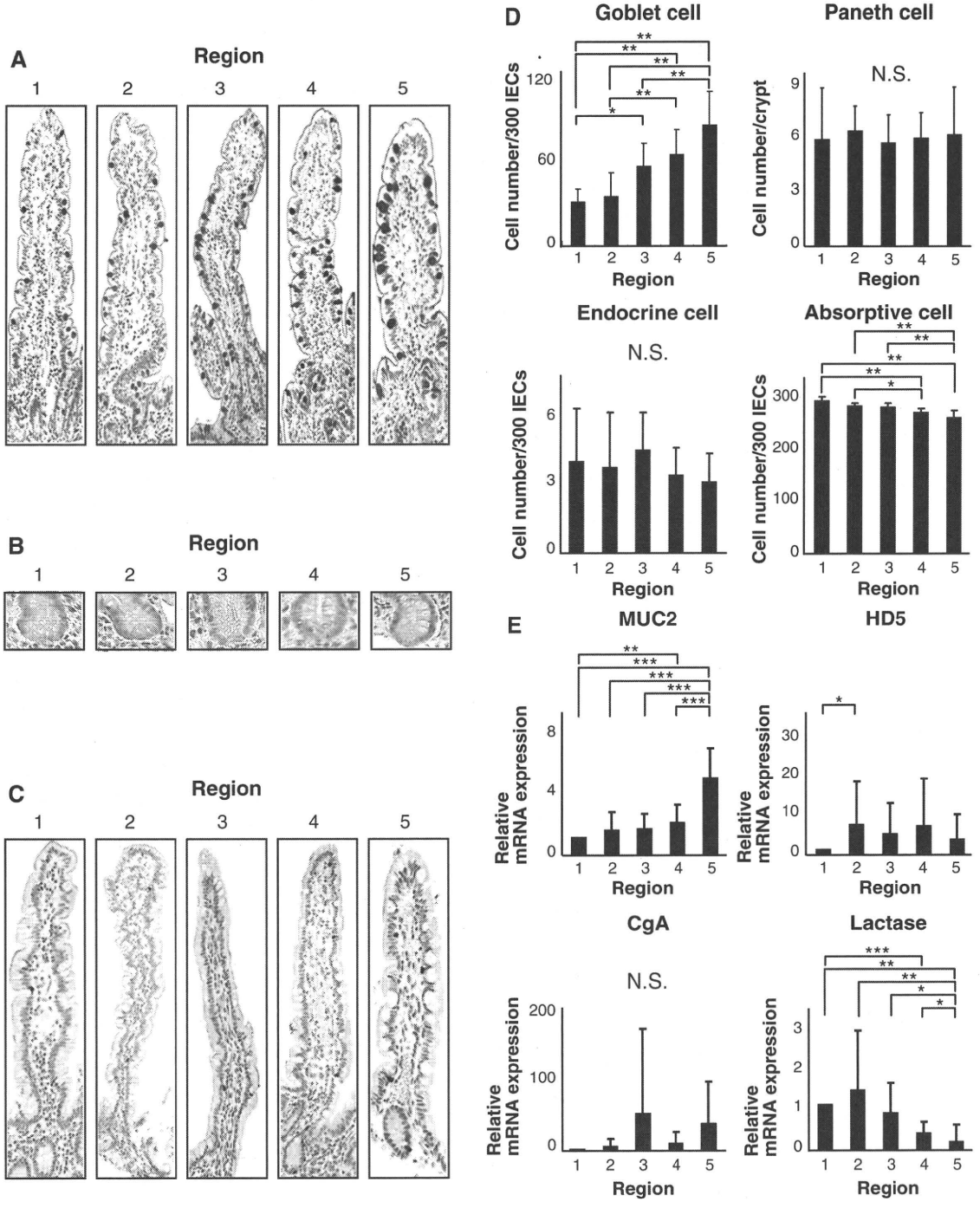

Fig. 2 Cell formations in the villus and the expression of phenotypic genes throughout the human small intestine. **a** Periodic acid-Schiff (PAS)-stained sections in each region (×10). Goblet cells were counted as PAS-positive cells. **b** H&E-stained sections of the crypt base in each region (×20). Paneth cells were counted as acidophilic granular cells. **c** CgA-immunostained sections of biopsy specimens (×10). CgA-positive cells are defined as endocrine cells. **d** Goblet cells were counted per 300 epithelial cells. Paneth cells were counted per crypt. Endocrine cells were counted as CgA-positive cells per 300 epithelial cells. The absorptive cell number was calculated by subtracting goblet cell and CgA-positive cell numbers from the total number. The number of each cell type is compared in each region ($*P < 0.05$, $**P < 0.01$, $n = 10$). **e** Relative mRNA expression of MUC2, representing goblet cells increased from proximal to distal regions in the human small intestine. Relative mRNA expression of HD5, representing Paneth cells, and CgA, representing enteroendocrine cells, was constant throughout the small intestine. Relative mRNA expression of lactase, representing absorptive cells, decreased from proximal to distal regions ($*P < 0.05$, $**P < 0.01$, $***P < 0.001$, $n = 10$). *IECs* Intestinal epithelial cells

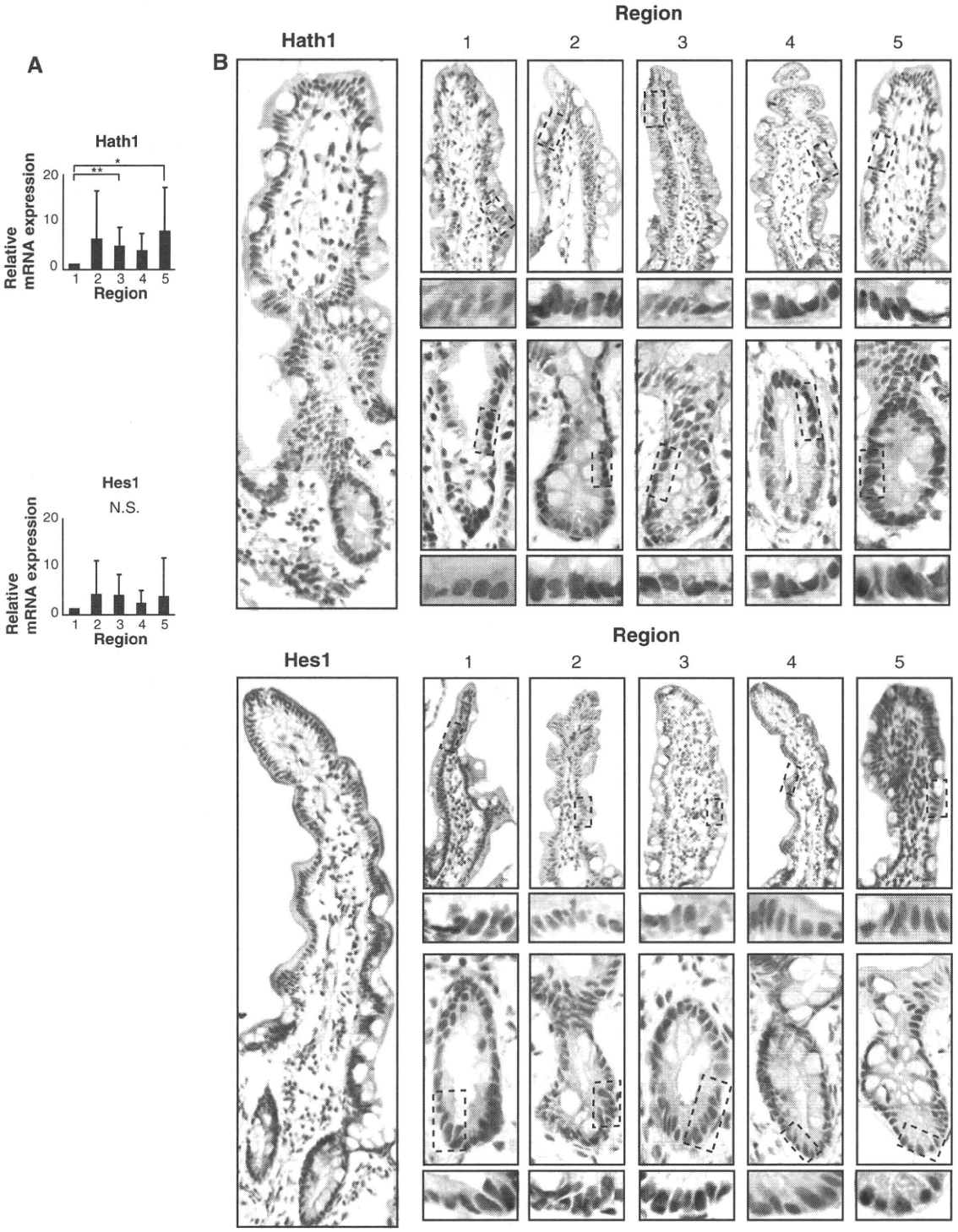

Fig. 3 Regional variation of Hath1 and Hes1 expression. **a** Quantitative real-time polymerase chain reaction (PCR) of Hath1 and Hes1 in the human small intestine. Relative mRNA expression of Hath1 increased from proximal to distal regions in the human small intestine ($*P < 0.05$, $**P < 0.01$, $n = 10$). Hes1 was constant throughout the small intestine (differences not significant, $P > 0.05$, $n = 10$). **b** *Upper panels* are Hath1-immunostained sections of biopsy specimens in each region (×20). In the villus, Hath1 expression increases from proximal to distal regions, while in the crypt, Hath1 is constantly expressed throughout the small intestine. The *left panel* shows Hath1 expression in the whole villus in region 5 (×10). *Lower panels* are Hes1-immunostained sections of biopsy specimens in each region (×20). A section of each picture is shown at high magnification (×40). Hes1 is expressed only in the crypt throughout the small intestine, and its expression is constant. The *left panel* shows Hes1 expression in the entire villus in region 4 (×10)

were constant throughout the small intestine. In the villi, however, Hath1-positive cells increased toward region 5 (Supplemental Fig. 2). These results indicated that the longitudinal regulation of Hath1 expression in the villi was independent of Hes1 expression via the Notch signal.

Increased Klf4 expression toward the terminal ileum affects the increase of goblet cells

The question remained, however, of why the increased Hath1 expression affected only goblet cells, because Hath1 has the potential to promote the differentiation of all secretory lineages, including goblet cells, Paneth cells, and enteroendocrine cells [17]. We therefore assumed that the increase in goblet cell number might be affected by another factor in addition to Hath1 expression. We considered Klf4 to be a likely candidate, because this gene is considered essential for the differentiation only of goblet cells among the four types of IECs, on the basis of previous reports that Klf4-deficient mice showed a defect of goblet cells [23]. We found that Klf4 was increased gradually toward the terminal ileum, with region 5 showing a significantly higher level than region 2 in the same way as Hath1 expression (Fig. 4a). Interestingly, the localization of Klf4-positive cells in region 1 was restricted to the top of the villi and the base of the crypts, with different localization from Hath1. However, toward the terminal ileum, Klf4-positive cells migrated from the top of the villi (Fig. 4b). The number of Klf4-positive cells was also increased in the villi, except for the crypts (Supplemental Fig. 2) Consequently all goblet cells in the villi came to coexpress Klf4 with Hath1 in parallel with the increase of goblet cells, especially in region 5 (Supplemental Fig. 3).

Subsequently, we hypothesized that the goblet cell formation along the small intestine might be regulated by an encounter between Hath1 and Klf4 independent of the Notch signal, different from that of the crypt–villus axis (Fig. 4c).

Klf4 suppresses the phenotypic gene expression for Paneth cells, while Hath1 upregulates phenotypic genes for both goblet and Paneth cells

To verify our hypothesis, we first confirmed the function of Hath1 and Klf4 genes with LS174T cells, in which HD5 and HD6 genes are expressed, as in the small intestine, because the cells derived from human small-intestinal epithelial cells were not available.

Forced expression of the Hath1 gene alone led to the increased expression of phenotypic genes for goblet cells and Paneth cells, suggesting that Hath1 might have the potential to induce all secretory lineages (Fig. 5a). Although Hath1 induced Klf4 gene expression slightly (Fig. 5a), silencing of the Hath1 gene by siRNA (small interfering RNA) treatment showed no alteration of Klf4 gene expression (data not shown), suggesting that Klf4 expression might be almost independent of Hath1 gene expression.

We next assessed the effect of goblet cell gene expression on the forced expression of the Klf4 gene alone because it has not been known whether Klf4 has the potential to express the phenotypic genes of goblet cells. We found that Klf4 gene expression showed slight induction of the MUC2 gene without induction of the endogenous Hath1 gene (Fig. 5b). However, TFF3 was not induced by Klf4 expression alone (Fig. 5b), suggesting that Klf4 might have some potential to induce the phenotypic gene expression of goblet cells. Interestingly, Klf4 suppressed both HD5 and HD6 gene expression, suggesting that Klf4 has the potential to suppress the phenotypic gene expression of Paneth cells (Fig. 5b).

Coexpression of Hath1 and Klf4 simultaneously promotes an increase of the phenotypic expression of goblet cells and a decrease of that for Paneth cells

We next asked how the coexpression of Hath1 and Klf4 in the terminal ileum is related to the increase of goblet cells. Hath1 expression alone resulted in the increased phenotypic gene expression of both goblet and Paneth cells (Fig. 6). We also assessed the effect of treatment by DOX on the additive Klf4 expression. Interestingly, Klf4 expression produced a decrease of Paneth cell phenotypic gene expression with no effect on the expression of goblet cell phenotypic genes induced by Hath1 (Fig. 6). Consequently, Klf4 might play a role in the direction of Hath1 function from Paneth cells to goblet cells, resulting in the increase of goblet cell phenotypic gene expression in the terminal ileum.

TFF3-positive goblet cells are increased in the terminal ileum of the human intestine

Finally, we assessed whether TFF3 expression was actually increased toward the terminal ileum in the human small intestine. Real-time PCR revealed an increase of TFF3 gene expression in the terminal ileum (Fig. 7a). Interestingly, TFF3 immunohistochemistry showed that some goblet cells did not include TFF3 in the jejunum and that TFF3-positive goblet cells increased toward the terminal ileum (Fig. 7b), suggesting that the encounter of Hath1 and Klf4 in the terminal ileum might specifically promote the differentiation and phenotypic gene expression of goblet cells.

Taken together, the increased Hath1 and Klf4 in the villi of terminal ileum resulted in the acceleration of goblet cell

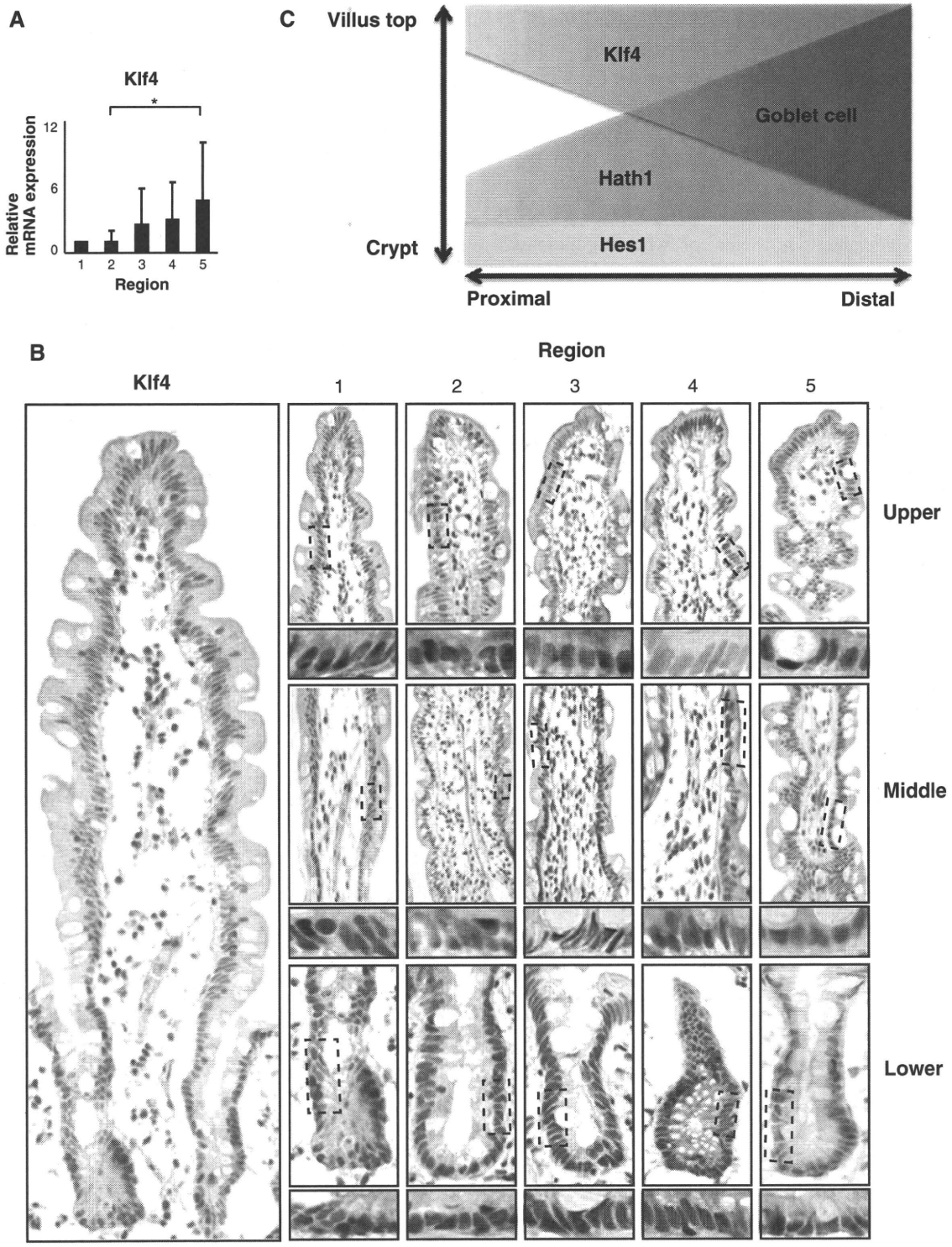

Fig. 4 Regional variation of Klf4 expression. **a** Quantitative real-time PCR of Klf4 in the human small intestine. Relative mRNA expression of Klf4 increased from proximal to distal regions ($*P < 0.05$, $n = 10$). **b** Klf4-immunostained sections of biopsy specimens in each region (×20). A section of each picture is shown at high magnification (×40). At the apex of villi, Klf4 is expressed in the nuclei in all cells, and Klf4 expression at the top of the villus is constant throughout the small intestine. In the middle part of the villus, Klf4 expression increases from proximal to distal regions with increasing goblet cell number. In the crypt, Klf4 is constantly expressed in a few cells from proximal to distal regions. The *left panel* shows Klf4 expression in the whole villus in region 1 (×10). **c** Schematic representation of the longitudinal regulation of goblet cell formation throughout the small intestine by the localization of Hath1 and Klf4

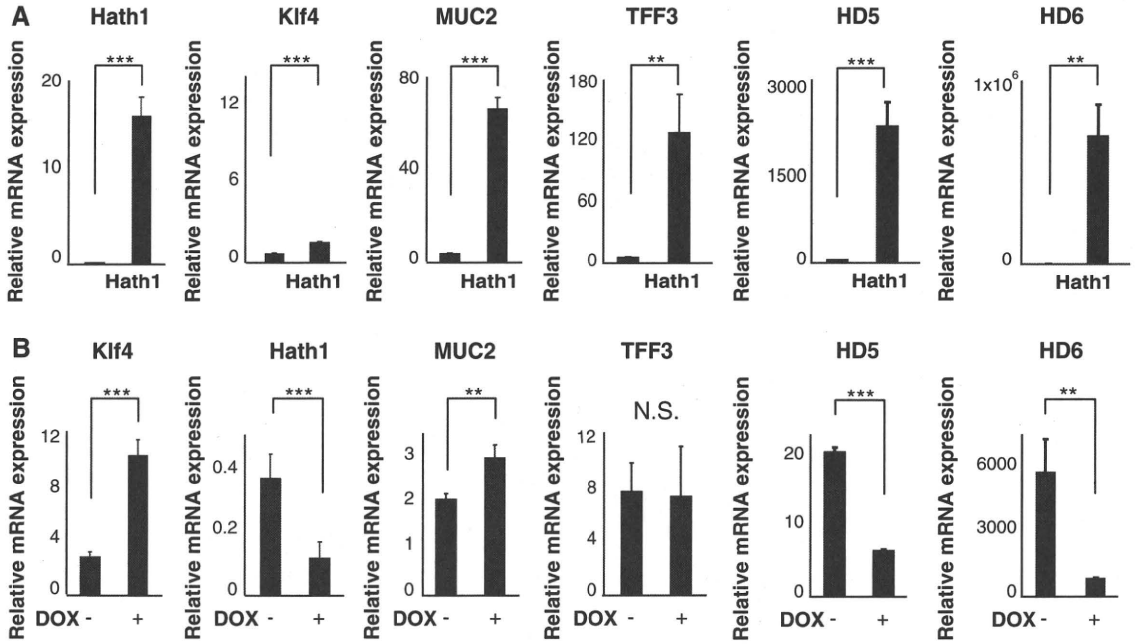

Fig. 5 Phenotype genes are regulated by Hath1 and Klf4. **a** Quantitative real-time PCR of phenotypic genes in cells forced to express Hath1 using a lentivirus infection system. Relative mRNA of Hath1, Klf4, MUC2, TFF3, HD5, and HD6 expression was elevated (**$P < 0.01$, ***$P < 0.001$, $n = 3$). **b** Quantitative real-time PCR of phenotypic genes in cells that were programmed in a Tet-On system to express Klf4 genes by treatment with doxycycline (*DOX*). Both HD5 and HD6 expressions were significantly decreased by Klf4 (**$P < 0.01$, ***$P < 0.001$, $n = 3$) (×10)

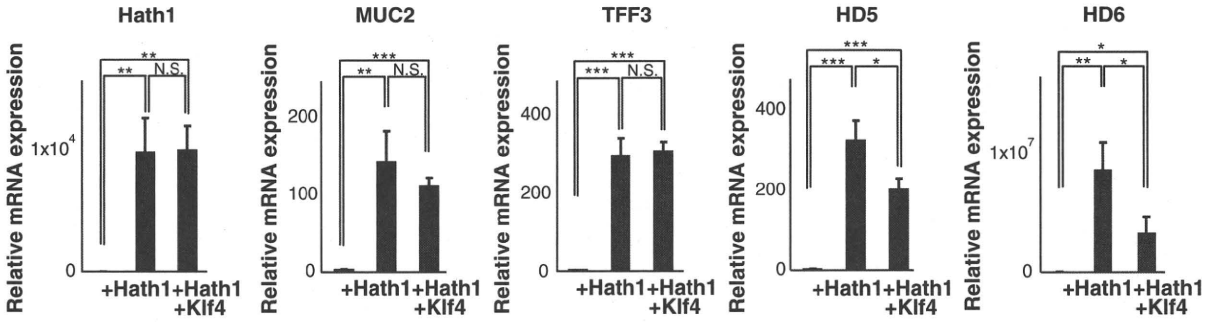

Fig. 6 Coexpression of Hath1 and Klf4 simultaneously promotes an increase in the phenotypic expression of goblet cells and a decrease in that for Paneth cells. Quantitative real-time PCR of phenotypic gene expression in LS174T Tet-On Klf4 cells under forced expression of the Hath1 gene by Hath1-lentivirus. Hath1 alone showed an increase in all genes. Klf4 expression by treatment with DOX under forced expression of Hath1 showed the suppression of HD5 and HD6 expressions induced by Hath1 (*$P < 0.05$, **$P < 0.01$, ***$P < 0.001$, $n = 3$)

differentiation and phenotypic gene expression, while the invariable number of Paneth cells throughout small intestine was maintained as a result of the invariable formation of Hath1-, Klf4- and Hes1-positive cells in the crypts (Fig. 7c) (Supplemental Fig. 2).

Discussion

This study has revealed, for the first time, the longitudinal regulation of the small intestine in the same person in an "alive environment" using mapping biopsy specimens collected by DBE. The most advantageous point of mapping biopsy by DBE was its utility for assessing the basic structure and cell formation of each region in the same small intestine, because the individual differences in villus size, cell formation, and gene expression in the operative tissue could be considered to elucidate regional regulation.

Surprisingly, the villus size did not change throughout an individual human's small intestine, although it has been reported that villus size decreases toward the ileum in rats [26]. Villus size in the human small intestine has often been measured in either anatomical tissue or operative tissue in which individual differences and the tissue

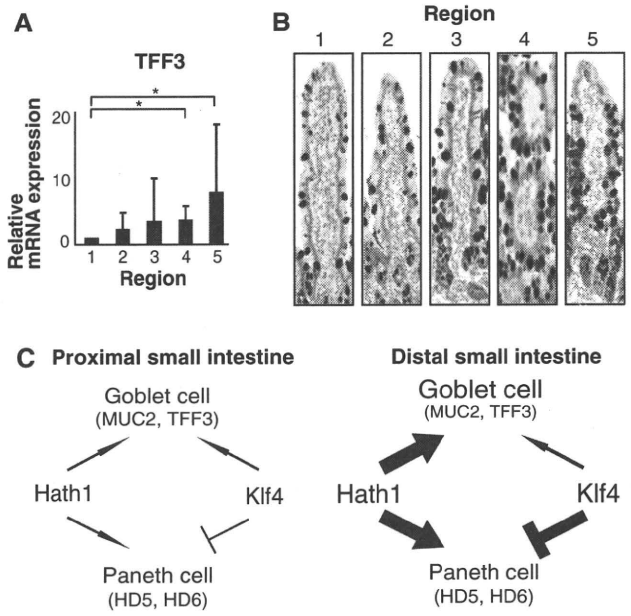

Fig. 7 Regional variation of TFF3 expression. **a** Quantitative real-time PCR of TFF3. Relative mRNA expression of TFF3 increases from proximal to distal regions in the human small intestine ($*P < 0.05$, $n = 10$). **b** TFF3-immunostained sections (×10). In the proximal region, TFF3 is found in some goblets, while on the distal side, TFF3 is found in all goblets and overflows outside the goblets. **c** Schematic representation of the functional regulation between Hath1 and Klf4 for longitudinal cell formation and gene expression throughout the human small intestine. In the terminal ileum, increased Klf4 offsets the differentiation into Paneth cells induced by increased Hath1 in the villi, resulting in maintaining the Paneth cell number throughout the human small intestine. In contrast, increased Klf4 and Hath1 induce differentiation into goblet cells

damage caused by the time lag during tissue fixation were not considered in the analysis of the basic structure of the human small intestine. Because there are few reports regarding human villus size, especially in biopsy specimens [27], more precise analysis of the regulation of villus size, which might be related to absorptive function, is necessary.

Another intriguing finding of this study is that the statistical analysis of MUC2 and lactase gene expression showed a regional distinction between regions 1 and 4 but not between regions 1 and 3. Moreover, the statistical analysis of gene expression showed a distinction between regions 1 and 2 for HD5, and between regions 2 and 5 for Klf4, indicating that the regional borderline is different for each phenotype. It has been commonly accepted that the small intestine is divided into the jejunum and ileum, as the proximal two-fifths and the distal three-fifths of the small intestine, respectively [28]; however, significant differences between these regions have never been elucidated. This is the first report to show that the regional expression of each gene in human small intestine differs from the classical division. More detailed global analysis of genes expressed in each region of the human small intestine might lead to an elucidation of the regional regulation of small-intestinal function.

Most importantly, the present study also shows that the longitudinal goblet cell and Paneth cell distribution in the villi along the human small intestine is regulated by the localization of Klf4 and Hath1, which increases the number of goblet cells toward the terminal ileum in contrast with no apparent alteration of Paneth cells. Although both Hath1 and Klf4 are essential for goblet cell differentiation, the relationship between Hath1 and Klf4 has not been elucidated precisely. Klf4 has generally been considered to be downstream of Hath [1, 23]; however, we showed different localizations of these proteins. How Hath1 and Klf4 are increased independently toward the terminal ileum might be very important for the regulation of cell formation, which is related to the regional function of the small intestine. It is known that the Notch signal regulates the differentiation of IECs in the villi [14], but the present study suggested that the Notch signal did not affect the regulation of longitudinal cell formation throughout the human small intestine. Therefore, another system that regulates longitudinal cell formation might determine regional function. Although it has been reported that Math1, the mouse homolog of Hath1, was expressed only in secretory cells in mice, the present study showed that Hath1 was expressed in all cells of the villi in the terminal ileum. However, the longitudinal regulation of Math1 in the mouse small intestine has not been elucidated, and the possibility remains that the longitudinal regulation of the small intestine is conserved among species.

Another important aspect of the encounter between Hath1 and Klf4 is the directional decision for goblet cell differentiation into three secretory lineages. Hath1 has the potential to promote the differentiation toward three types of secretory cells [17], but how the goblet cells differentiate from Hath1-positive cells remains unknown. It has been reported that Gfi1 distinguishes Paneth cells and goblet cells from secretory cells [29], but it is not known how the differentiation program branches into Paneth cells and goblet cells. The present study showed that Klf4 has the potential not only to promote some goblet cell gene expression but also to suppress, selectively, the Hath1 function that promotes the Paneth cell phenotype. However, a more detailed mechanism should be elucidated using human small-intestinal epithelial cells.

The longitudinal formation of the cell lineages other than goblet cells was also identified. Interestingly, the numbers of Paneth cells and endocrine cells were invariable throughout the small intestine. The number of Paneth cells and the expression of antimicrobial peptides have been considered to increase toward the terminal ileum according to the propagation of intestinal bacterial flora

[30]. However, the present study showed no alteration in the number of Paneth cells or the expression of HD5 in individuals, as indicated by the constant expression of Hath1, Hes1, and Klf4 in the crypts throughout the small intestine. Because an abnormality of HD5 gene expression has been the focus of the functional pathology of Crohn's disease [31, 32], these data might be important for comparing HD5 gene expression in each region of the intestine in Crohn's disease for gaining a more detailed understanding of the pathology and for developing a diagnostic indicator.

In summary, we have revealed for the first time the molecular regulation of the basic longitudinal structure of the human small intestine by using mapping biopsy of the entire small intestine. The regulation of longitudinal cell formation in the small intestine is suggested to differ from that of crypt–villus axial cell formation, indicating that the situation of both axes should be considered in the regulation of cell formation in the small intestine to understand the determination of cell fate in both normal and pathological small intestine. Greater understanding of the basic regulation of cell formation in the human small intestine might be useful for the comparison of small-intestinal diseases, including unknown lesions, in order to elucidate further their pathologies and to exploit new therapies.

Acknowledgments This study was supported in part by Grants-in-Aid for Scientific Research 19209027, 21590803, 21790651, and 21790653, from the Japanese Ministry of Education, Culture, Sports, Science and Technology; and by grants from JFE (The Japanese Foundation for Research and Promotion of Endoscopy) and the Japan Foundation for Applied Enzymology; and by Intractable Diseases, Health and Labor Sciences research grants from the Japanese Ministry of Health, Labor and Welfare.

References

1. Iddan G, Meron G, Glukhovsky A, Swain P. Wireless capsule endoscopy. Nature. 2000;405:417.
2. Appleyard M, Fireman Z, Glukhovsky A, Jacob H, Shreiver R, Kadirkamanathan S, Lavy A, Lewkowicz S, Scapa E, Shofti R, Swain P, Zaretsky A. A randomized trial comparing wireless capsule endoscopy with push enteroscopy for the detection of small-bowel lesions. Gastroenterology. 2000;119:1431–8.
3. Yamamoto H, Kita H. Double-balloon endoscopy. Curr Opin Gastroenterol. 2005;21:573–7.
4. Yamamoto H, Kita H. Enteroscopy. J Gastroenterol. 2005;40:555–62.
5. Yamamoto H. Double-balloon endoscopy. Clin Gastroenterol Hepatol. 2005;3:S27–9.
6. Pasha SF, Leighton JA, Das A, Harrison ME, Decker GA, Fleischer DE, Sharma VK. Double-balloon enteroscopy and capsule endoscopy have comparable diagnostic yield in small-bowel disease: a meta-analysis. Clin Gastroenterol Hepatol. 2008;6:671–6.
7. Mitsui K, Tanaka S, Yamamoto H, Kobayashi T, Ehara A, Yano T, Goto H, Nakase H, Matsui T, Iida M, Sugano K, Sakamoto C. Role of double-balloon endoscopy in the diagnosis of small-bowel tumors: the first Japanese multicenter study. Gastrointest Endosc. 2009;70:498–504.
8. Matsumoto T, Iida M, Matsui T, Yao T. Chronic nonspecific multiple ulcers of the small intestine: a proposal of the entity from Japanese gastroenterologists to Western enteroscopists. Gastrointest Endosc. 2007;66:S99–107.
9. Chung YC, Kim YS, Shadchehr A, Garrido A, Macgregor IL, Sleisenger MH. Protein digestion and absorption in human small intestine. Gastroenterology. 1979;76:1415–21.
10. Macdonald TT, Monteleone G. Immunity, inflammation, and allergy in the gut. Science. 2005;307:1920–5.
11. Badman MK, Flier JS. The gut and energy balance: visceral allies in the obesity wars. Science. 2005;307:1909–14.
12. Backhed F, Ley RE, Sonnenburg JL, Peterson DA, Gordon JI. Host–bacterial mutualism in the human intestine. Science. 2005;307:1915–20.
13. Clevers H. Wnt/beta-catenin signaling in development and disease. Cell. 2006;127:469–80.
14. Fre S, Huyghe M, Mourikis P, Robine S, Louvard D, Artavanis-Tsakonas S. Notch signals control the fate of immature progenitor cells in the intestine. Nature. 2005;435:964–8.
15. He XC, Zhang J, Tong WG, Tawfik O, Ross J, Scoville DH, Tian Q, Zeng X, He X, Wiedemann LM, Mishina Y, Li L. BMP signaling inhibits intestinal stem cell self-renewal through suppression of Wnt-beta-catenin signaling. Nat Genet. 2004;36:1117–21.
16. Crosnier C, Stamataki D, Lewis J. Organizing cell renewal in the intestine: stem cells, signals and combinatorial control. Nat Rev Genet. 2006;7:349–59.
17. Yang Q, Bermingham NA, Finegold MJ, Zoghbi HY. Requirement of Math1 for secretory cell lineage commitment in the mouse intestine. Science. 2001;294:2155–8.
18. Tsuchiya K, Nakamura T, Okamoto R, Kanai T, Watanabe M. Reciprocal targeting of Hath1 and beta-catenin by Wnt glycogen synthase kinase 3beta in human colon cancer. Gastroenterology. 2007;132:208–20.
19. Okamoto R, Tsuchiya K, Nemoto Y, Akiyama J, Nakamura T, Kanai T, Watanabe M. Requirement of Notch activation during regeneration of the intestinal epithelia. Am J Physiol Gastrointest Liver Physiol. 2009;296:G23–35.
20. Silk DB, Webb JP, Lane AE, Clark ML, Dawson AM. Functional differentiation of human jejunum and ileum: a comparison of the handling of glucose, peptides, and amino acids. Gut. 1974;15:444–9.
21. Wehkamp J, Chu H, Shen B, Feathers RW, Kays RJ, Lee SK, Bevins CL. Paneth cell antimicrobial peptides: topographical distribution and quantification in human gastrointestinal tissues. FEBS Lett. 2006;580:5344–50.
22. George MD, Wehkamp J, Kays RJ, Leutenegger CM, Sabir S, Grishina I, Dandekar S, Bevins CL. In vivo gene expression profiling of human intestinal epithelial cells: analysis by laser microdissection of formalin fixed tissues. BMC Genomics. 2008;9:209.
23. Katz JP, Perreault N, Goldstein BG, Lee CS, Labosky PA, Yang VW, Kaestner KH. The zinc-finger transcription factor Klf4 is required for terminal differentiation of goblet cells in the colon. Development. 2002;129:2619–28.
24. Aragaki M, Tsuchiya K, Okamoto R, Yoshioka S, Nakamura T, Sakamoto N, Kanai T, Watanabe M. Proteasomal degradation of Atoh1 by aberrant Wnt signaling maintains the undifferentiated state of colon cancer. Biochem Biophys Res Commun. 2008;368:923–9.
25. Oshima S, Nakamura T, Namiki S, Okada E, Tsuchiya K, Okamoto R, Yamazaki M, Yokota T, Aida M, Yamaguchi Y, Kanai T, Handa H, Watanabe M. Interferon regulatory factor 1 (IRF-1) and IRF-2 distinctively up-regulate gene expression and

production of interleukin-7 in human intestinal epithelial cells. Mol Cell Biol. 2004;24:6298–310.
26. Fernandez-Estivariz C, Gu LH, Gu L, Jonas CR, Wallace TM, Pascal RR, Devaney KL, Farrell CL, Jones DP, Podolsky DK, Ziegler TR. Trefoil peptide expression and goblet cell number in rat intestine: effects of KGF and fasting-refeeding. Am J Physiol Regul Integr Comp Physiol. 2003;284:R564–73.
27. Wood GM, Gearty JC, Cooper BT. Small bowel morphology in British Indian and Afro-Caribbean subjects: evidence of tropical enteropathy. Gut. 1991;32:256–9.
28. Grant JP. Anatomy and physiology of the luminal gut: enteral access implications. JPEN J Parenter Enteral Nutr. 2006;30: S41–6.
29. Shroyer NF, Wallis D, Venken KJ, Bellen HJ, Zoghbi HY. Gfi1 functions downstream of Math1 to control intestinal secretory cell subtype allocation and differentiation. Genes Dev. 2005;19: 2412–7.
30. Williams RE. Benefit and mischief from commensal bacteria. J Clin Pathol. 1973;26:811–8.
31. Wehkamp J, Salzman NH, Porter E, Nuding S, Weichenthal M, Petras RE, Shen B, Schaeffeler E, Schwab M, Linzmeier R, Feathers RW, Chu H, Lima H Jr, Fellermann K, Ganz T, Stange EF, Bevins CL. Reduced Paneth cell alpha-defensins in ileal Crohn's disease. Proc Natl Acad Sci USA. 2005;102:18129–34.
32. Wehkamp J, Wang G, Kubler I, Nuding S, Gregorieff A, Schnabel A, Kays RJ, Fellermann K, Burk O, Schwab M, Clevers H, Bevins CL, Stange EF. The Paneth cell alpha-defensin deficiency of ileal Crohn's disease is linked to Wnt/Tcf-4. J Immunol. 2007;179:3109–18.

Upregulated IL-7 Receptor α Expression on Colitogenic Memory CD4$^+$ T Cells May Participate in the Development and Persistence of Chronic Colitis

Tamako Shinohara,*[,1] Yasuhiro Nemoto,*[,1] Takanori Kanai,[†] Kaori Kameyama,* Ryuichi Okamoto,* Kiichiro Tsuchiya,* Tetsuya Nakamura,* Teruji Totsuka,* Koichi Ikuta,[‡] and Mamoru Watanabe*

We have previously demonstrated that IL-7 is essential for the persistence of colitis as a survival factor of colitogenic IL-7Rα–expressing memory CD4$^+$ T cells. Because IL-7Rα is broadly expressed on various immune cells, it is possible that the persistence of colitogenic CD4$^+$ T cells is affected by other IL-7Rα–expressing non-T cells. To test this hypothesis, we conducted two adoptive transfer colitis experiments using IL-7Rα$^{-/-}$ CD4$^+$CD25$^-$ donor cells and IL-7Rα$^{-/-}$ × RAG-2$^{-/-}$ recipient mice, respectively. First, IL-7Rα expression on colitic lamina propria (LP) CD4$^+$ T cells was significantly higher than on normal LP CD4$^+$ T cells, whereas expression on other colitic LP immune cells, (e.g., NK cells, macrophages, myeloid dendritic cells) was conversely lower than that of paired LP cells in normal mice, resulting in predominantly higher expression of IL-7Rα on colitogenic LP CD4$^+$ cells, which allows them to exclusively use IL-7. Furthermore, RAG-2$^{-/-}$ mice transferred with IL-7Rα$^{-/-}$ CD4$^+$CD25$^-$ T cells did not develop colitis, although LP CD4$^+$ T cells from mice transferred with IL-7Rα$^{-/-}$ CD4$^+$CD25$^-$ T cells were differentiated to CD4$^+$ CD44^{high}CD62L$^-$ effector-memory T cells. Finally, IL-7Rα$^{-/-}$ × RAG-2$^{-/-}$ mice transferred with CD4$^+$CD25$^-$ T cells developed colitis similar to RAG-2$^{-/-}$ mice transferred with CD4$^+$CD25$^-$ T cells. These results suggest that IL-7Rα expression on colitogenic CD4$^+$ T cells, but not on other cells, is essential for the development of chronic colitis. Therefore, therapeutic approaches targeting the IL-7/IL-7R signaling pathway in colitogenic CD4$^+$ T cells may be feasible for the treatment of inflammatory bowel diseases. *The Journal of Immunology*, 2011, 186: 2623–2632.

Inflammatory bowel disease (IBD) is characterized by idiopathic chronic intestinal inflammation, which commonly takes a persistent course with lifelong recurrence (1–4). According to current understanding, IBD is caused by inappropriate responses of the activated immune system to intestinal commensal bacteria in patients with a genetically susceptible background. Above all, effector CD4$^+$ T cells including Th1, Th2, and Th17 are highlighted in the pathogenesis of IBD, because some groups have reported the association between genes involved in the Th17/IL-23 pathway and IBD (5, 6). Alternatively, we have investigated the possibility that long-lived memory CD4$^+$ T cells are the main cause of the persistence of IBD and have proved the importance of IL-7 for the maintenance system of memory CD4$^+$ T cells in chronic colitis (7).

IL-7 is a stromal cell-derived cytokine that is secreted by fetal liver cells, stromal cells in the bone marrow, and the thymus and other epithelial cells, including intestinal goblet cells (8, 9). Recently, IL-7 has emerged as a critical key cytokine involved in controlling the survival of peripheral resting CD4$^+$ T cells, including naive and memory cells, but not effector cells, and their homeostatic turnover proliferation (8–15). The effect of IL-7 on CD4$^+$ T cells is controlled by the expression of the specific receptors for IL-7, the state of differentiation of the T cells, the available concentration of IL-7, and whether there is concomitant TCR signaling (16, 17).

In contrast to the role of IL-7 in naive and memory CD4$^+$ T cells in the resting state, the pathologic role of IL-7 in chronic immune-mediated diseases, such as autoimmune diseases and IBD, remains largely unclear. We have previously demonstrated that 1) IL-7 is constitutively produced by intestinal epithelial cells, especially by goblet cells (18); 2) IL-7 transgenic mice developed chronic colitis that mimicked histopathologic characteristics of human IBD (19); 3) colonic lamina propria (LP) CD4$^+$IL-7Rα^{high} T cells in RAG-2$^{-/-}$ mice in which colitis was induced by adoptive transfer of CD4$^+$CD45RB^{high} T cells have characteristics of colitogenic memory T cells (20); 4) the selective elimination of CD4$^+$IL-7Rα^{high} T cells by administrating toxin-conjugated anti–IL-7Rα mAb completely ameliorated ongoing colitis in TCR-α–deficient mice (21); and 5) IL-7 is essential for the persistence of colitis by showing that IL-7$^{-/-}$ × RAG-1$^{-/-}$ mice transferred with colitogenic LP CD4$^+$ T cells did not develop colitis (22).

*Department of Gastroenterology and Hepatology, Graduate School, Tokyo Medical and Dental University, Tokyo 113-8519, Japan; [†]Division of Gastroenterology and Hepatology, Department of Internal Medicine, Keio University School of Medicine, Tokyo 160-8852, Japan; and [‡]Laboratory of Biological Protection, Department of Biological Responses, Institute for Virus Research, Kyoto University, Kyoto 606-8507, Japan

[1]T.S. and Y.N. contributed equally to this work.

Received for publication January 11, 2010. Accepted for publication December 14, 2010.

This work was supported in part by grants-in-aid for Scientific Research, Scientific Research on Priority Areas, Exploratory Research and Creative Scientific Research from the Japanese Ministry of Education, Culture, Sports, Science and Technology; the Japanese Ministry of Health, Labor and Welfare; the Japan Medical Association; the Foundation for Advancement of International Science; the Keio Medical Science Foundation; and the Research Fund of Mitsukoshi Health and Welfare Foundation.

Address correspondence to Dr. Mamoru Watanabe, Department of Gastroenterology and Hepatology, Tokyo Medical and Dental University, 1-5-45 Yushima, Bunkyo-ku, Tokyo 113-8519, Japan. E-mail address: mamoru.gast@tmd.ac.jp

The online version of this article contains supplemental material.

Abbreviations used in this article: IBD, inflammatory bowel disease; LP, lamina propria; MFI, mean fluorescence intensity; SP, spleen; T_{EM}, effector-memory T; Treg, regulatory T cell; TSLP, thymic stromal lymphopoietin; WT, wild type.

www.jimmunol.org/cgi/doi/10.4049/jimmunol.1000057

We hypothesize that the dysregulated IL-7/IL-7Rα pathway is critically involved in the pathogenesis of animal models of chronic colitis and human IBD, although IL-7 seems to be strictly regulated at a constant level as a homeostatic cytokine to maintain the number of $CD4^+$ memory T cells in the body.

IL-7R consists of the α-chain (CD127) and the cytokine receptor γ-chain (IL-2Rγ; CD132), which is shared by the common γ-chain family cytokines (IL-2, IL-4, IL-9, IL-15, and IL-21) (14, 15). Because IL-7Rα is broadly expressed on $CD4^+$ T and NK cells, macrophages, dendritic cells, fibroblasts, and epithelial cells (14, 15), the persistence of colitogenic memory $CD4^+$ T cells may be affected by those cells in the form of "IL-7 competition". To assess this possibility, we attempted to clarify the link between the expression of IL-7Rα on various cells in the whole body in normal and colitic conditions and the pathogenesis of chronic colitis. In this study, we prove that IL-7Rα expression on $CD4^+$ T cells, but not on other cells (NK cells, granulocytes, macrophages, and dendritic cells), is essential for the development of colitis by use of an adoptive transfer colitis model using IL-7Rα$^{-/-}$ donor cells and IL-7Rα$^{-/-}$ × RAG-2$^{-/-}$ recipient mice.

Materials and Methods

Animals

Female C57BL/6 mice were purchased from Japan CLEA (Tokyo, Japan). C57BL/6-background RAG-2$^{-/-}$ mice were obtained from Taconic Farms (Hudson, NY). C57BL/6-background IL-7Rα$^{-/-}$ mice have been described previously (23). IL-7Rα$^{-/-}$ mice were intercrossed with RAG-2$^{-/-}$ mice to generate IL-7Rα$^{-/-}$ × RAG-2$^{-/-}$ mice in the Animal Care Facility of Tokyo Medical and Dental University. Mice were maintained under specific pathogen-free conditions in the Animal Care Facility of Tokyo Medical and Dental University. Female donors and recipients were used at 6-12 wk of age. All experiments were approved by the regional animal study committees and were performed according to institutional guidelines and home office regulations.

Purification of T cell subsets

$CD4^+$ T cells were isolated from spleen cells of IL-7Rα$^{-/-}$ or C57BL/6 mice using the anti-CD4 (L3T4)-MACS system (Miltenyi Biotec, Auburn, CA) according to the manufacturer's instructions. Enriched $CD4^+$ T cells (96–97% pure, as estimated by FACSCalibur [Becton Dickinson, Sunnyvale, CA]) were then labeled with PE-conjugated anti-mouse CD4 (RM4-5; BD Pharmingen, San Diego, CA) and FITC-conjugated anti-CD25 (7D4; BD Pharmingen). Subpopulations of $CD4^+$ cells were generated by two-color sorting on a FACSAria (Becton Dickinson). All populations were >97.0% pure on reanalysis. To isolate LP $CD4^+$ T cells, the entire colon was opened longitudinally, washed with PBS, and cut into small pieces. The dissected mucosa was incubated with Ca^{2+}, Mg^{2+}-free HBSS containing 1 mM DTT (Sigma-Aldrich) for 45 min to remove mucus, then treated with 3.0 mg/ml collagenase (Worthington Biomedical, Freehold, NJ) for 2 to 3 h. The cells were subjected to Ficoll-Hypaque density gradient centrifugation (40%/75%). Enriched LP $CD4^+$ T cells were obtained by positive selection using anti-CD4 (L3T4) MACS magnetic beads. The resultant cells when analyzed by FACSCalibur contained >95% $CD4^+$ cells.

In vivo experimental design

The role of IL-7Rα in the development and persistence of murine chronic colitis was investigated through a series of in vivo experiments.

Experiment 1. To assess the necessity of IL-7Rα on donor $CD4^+$ cells in the development of colitis, we performed cell transfer experiments using wild type (WT) and IL-7Rα$^{-/-}$ mice as donors. RAG-2$^{-/-}$ mice were injected i.p. with 3×10^5 splenic $CD4^+CD25^-$ T cells obtained from normal 8-wk-old WT and IL-7Rα$^{-/-}$ mice. As a negative control, RAG-2$^{-/-}$ mice were transferred with $CD4^+CD25^-$ T cells (3×10^5) and $CD4^+CD25^+$ regulatory T cells (Tregs; 1×10^5).

Experiment 2. To assess the necessity of IL-7Rα expression on cells of recipient mice in the development of colitis, we transferred $CD4^+CD25^-$ T cells (3×10^5) obtained from WT mice into RAG-2$^{-/-}$ mice and IL-7Rα$^{-/-}$ × RAG-2$^{-/-}$ mice as recipients. The recipient mice were weighed immediately after transfer and then three times per week. They were also observed for clinical signs such as hunched posture, piloerection, diarrhea, and blood in the stool. Mice were sacrificed 11 wk after transfer for experiment 1 and 8 wk after transfer for experiment 2 and assessed for a clinical score (24) that is the sum of four parameters as follows: hunching and wasting, 0 or 1; colon thickening, 0–3 (0, no colon thickening; 1, mild thickening; 2, moderate thickening; 3, extensive thickening); and stool consistency, 0–3 (0, normal beaded stool; 1, soft stool; 2, diarrhea; 3, bloody stool) (24). To monitor the clinical signs during the observation period, the disease activity index is defined as the sum (0–5 points) of the parameters other than colon thickening.

Histologic examination

Tissue samples were fixed in PBS containing 10% neutral-buffered formalin. Paraffin-embedded sections (5 μm) were stained with H&E. Two tissue samples from the proximal and distal parts of the colon were prepared. The sections were analyzed without prior knowledge of the type of T cell reconstitution or treatment. The area most affected was graded by the number and severity of lesions. The mean degree of inflammation in the colon was calculated using a modification of a previously described scoring system (25) as the sum of three parameters: crypt elongation, 0–3; mononuclear cell infiltration, 0–3; and frequency of crypt abscesses.

Cytokine ELISA

To measure cytokine production, 1×10^5 LP $CD4^+$ T cells were cultured in 200 μl of culture medium at 37°C in a humidified atmosphere containing 5% CO_2 in 96-well plates (Costar, Cambridge, MA) precoated with 5 μg/ml hamster anti-mouse CD3ε mAb (145-2C11; BD Pharmingen) and 2 μg/ml hamster anti-mouse CD28 mAb (37.51; BD Pharmingen) in PBS overnight at 4°C (24). Culture supernatants were removed after 48 h and assayed for cytokine production. Cytokine concentrations were determined by specific ELISA per the manufacturer's recommendation (R&D Systems, Minneapolis, MN).

Flow cytometry

To detect the surface expression of various molecules, isolated splenocytes or LP mononuclear cells were preincubated with an FcγR-blocking mAb (CD16/32; 2.4G2; BD Pharmingen) for 20 min followed by incubation with specific FITC-, PE-, PECy5-, or biotin-labeled Abs for 30 min on ice. The following mAbs, other than biotin-conjugated anti-mouse IL-7Rα (A7R34; Immuno-Biological Laboratories (Takasaki Japan), were obtained from BD Pharmingen: anti-CD4 mAb (RM4-5), anti-CD25 mAb (7D4), anti-CD45RB mAb (16A), anti-CD62L (MEL-14), anti-CD44 mAb (IM7), anti-CD69 mAb (H1.2F3), and anti–Bcl-2 mAb (3F11). Biotinylated Abs were detected with PE-streptavidin. Standard two- or three-color flow cytometric analyses were obtained using the FACSCalibur with CellQuest software. Background fluorescence was assessed by staining with control-irrelevant isotype-matched mAbs. To analyze the TCR Vβ family repertoire, splenic cells were double-stained with PE-conjugated anti-CD4 mAb (RM4-5) and the following FITC-conjugated mAbs: Vβ2; KJ25, Vβ3; KT4, Vβ4; MR9-4, Vβ5; RR4-7, Vβ6; TR310, Vβ7; MR5-2, Vβ8.1/2; B21.14, Vβ8.3; MR10-2, Vβ9; B21.5, Vβ10; RR3-15, Vβ11; MR11-1, Vβ12; IN12.3, Vβ13; 14.2, Vβ14; and KJ23, Vβ17. All Abs were purchased from BD Pharmingen.

For intracellular staining of cytokines, $CD4^+$ T cells were cultured for 12 h with ionomycin (500 ng/ml), PMA (50 ng/ml), and BD GolgiPlug (1 μl/ml BD Pharmingen). After the stimulation, cells were collected and their surface molecules were stained. Cells were fixed using Cytofix/Cytoperm Kit (BD Pharmingen) and then stained with PE-conjugated anti–IL-17A mAb (TC11-18H10; BD Pharmingen) or FITC-conjugated anti–IFN-γ mAb (XMG1.2; BD Pharmingen) for 20 min (26).

Statistical analysis

We examined the normality of each group. If either group was not normally distributed, we assessed the difference between two groups using the Mann-Whitney U test. If both groups were normally distributed, we assessed the variance of population within each group using F test. With homoscedasticity of both populations, we assessed the difference between two groups using the Student t test. Without homoscedasticity, we assessed the difference using Welch's t test. We used the program Statcell for all statistical analysis Differences were considered to be statistically significant when $p < 0.05$.

Results

IL-7Rα is expressed on various immune cells in WT and colitic mice

To first assess the role of the IL-7/IL-7R signaling pathway in the development of chronic colitis, we analyzed the expression of

IL-7Rα on various immune compartments in colonic LP of normal C57BL/6 mice (normal mice) and colitic C57BL/6-RAG-2$^{-/-}$ mice previously transferred with WT CD4$^+$CD25$^-$ T cells (colitic mice). First, both normal and colitic LP CD3$^+$CD4$^+$ T cells highly expressed IL-7Rα, but the mean fluorescence intensity (MFI) of IL-7Rα expression on LP CD3$^+$CD4$^+$ T cells from colitic mice was significantly higher than in normal mice (Fig. 1*A*, 1*B*). Conversely, the MFIs of IL-7Rα expression on colitic LP CD3$^-$NK1.1$^+$ NK cells, CD11b$^+$Gr^{high} granulocytes, CD11b$^+$Gr$^{low/-}$ macrophages, and CD11b$^+$CD11c$^+$ myeloid dendritic cells were significantly downregulated compared with those from normal mice (Fig. 1*A*, 1*B*). In addition, there were no differences in the expression of IL-7Rα on CD3$^-$NKp46$^+$ NK22-like cells (27–29) and CD11b$^-$CD11c$^+$ lymphoid dendritic cells (Fig. 1*A*, 1*B*). These changes of IL-7Rα expression in LP cells of colitic mice resulted in the highest expression of IL-7Rα on CD3$^+$CD4$^+$ T cells as compared with that on other compartments (Fig. 1*B*), suggesting preferential use of IL-7 by CD3$^+$CD4$^+$ T cells in colitic conditions.

Naive CD4$^+$ T cells are retained in substantial numbers in spleens of IL-7Rα$^{-/-}$ mice

Given the evidence that various immune compartments constitutively express IL-7Rα, we next attempted to assess the role of IL-7Rα expression in the development of chronic colitis induced by adoptive transfer of CD4$^+$CD25$^-$ T cells obtained from age-matched WT or IL-7Rα$^{-/-}$ mice into RAG-2$^{-/-}$ mice. It was particularly interesting that the expression level of IL-7Rα on colitic LP CD3$^+$CD4$^+$ T cells was significantly higher than that of other compartments in colitic conditions (Fig. 1). Because it is also known that IL-7/IL-7R signaling is critically involved in T cell development in thymus and the periphery (9, 10), we first assessed phenotypic characteristics of splenic CD4$^+$ T cells in age-matched WT and IL-7Rα$^{-/-}$ mice before starting a series of adoptive transfer experiments. Consistent with previous reports (23, 30), the absolute cell number of CD3$^+$CD4$^+$ T cells recovered from spleen (SP) of IL-7Rα$^{-/-}$ mice was significantly lower than that of WT mice (data not shown). Although the ratio of naive (CD44$^{low/-}$CD62L$^+$) versus memory (CD44^{high}CD62L$^-$) T cells in SP of IL-7Rα$^{-/-}$ mice was markedly decreased compared with that of WT mice, a substantial number of naive CD4$^+$ T cells were retained in SP of IL-7Rα$^{-/-}$ mice (Fig. 2*A*). In addition, we confirmed that SP CD4$^+$ T cells of IL-7Rα$^{-/-}$ mice did not express IL-7Rα, and no differences in the expression of CD69, Foxp3, and CD25 were found between two groups (Fig. 2*A*). Of note, Bcl-2 expression in SP CD4$^+$ T cells of IL-7Rα$^{-/-}$ mice was significantly lower than that of WT mice ($p < 0.05$; Fig. 2*A*), which seemed to be consistent with previous reports that IL-7 is essential for survival of CD4$^+$ T cells (24). It was also possible that CD4$^+$CD25$^-$ donor T cells in SPs of IL-7Rα$^{-/-}$ mice retain restricted clonality of CD4$^+$ T cells because of the dysregulated differentiation of CD4$^+$ T cells in the thymus as compared with that in WT mice. To test this possibility, we compared TCR Vβ repertoires of SP CD4$^+$CD25$^-$ T cells from age-matched IL-7Rα$^{-/-}$ and WT mice. Flow cytometric analysis of these SP CD4$^+$ cells using a panel of 15 anti-Vβ mAbs showed that the major Vβ population was Vβ8.1/8.2 in both groups, and the only significant difference in Vβ repertoires between the groups was Vβ8.3 (Fig. 2*B*).

RAG-2$^{-/-}$ mice transferred with IL-7Rα$^{-/-}$ CD4$^+$CD25$^-$ T cells did not develop mild colitis

To then assess the role of the IL-7R signaling pathway in the development of chronic colitis, we used a chronic colitis model induced by adoptive transfer of SP CD4$^+$CD25$^-$ T cells from IL-7Rα$^{-/-}$ or control WT mice into RAG-2$^{-/-}$ recipients (Fig. 3*A*).

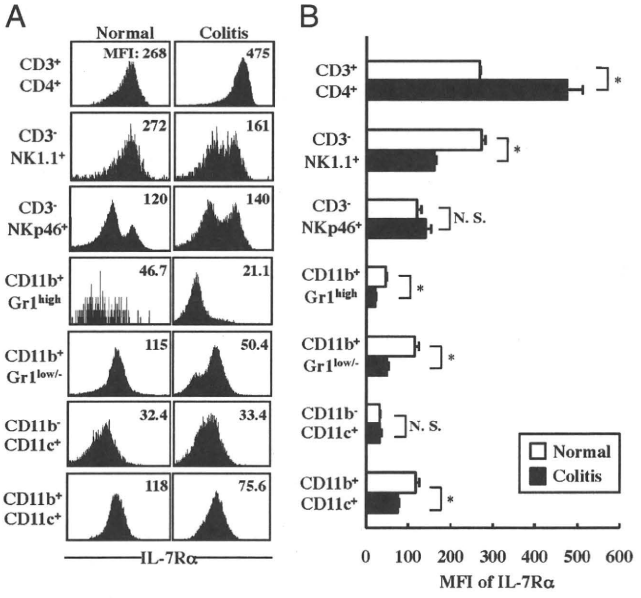

FIGURE 1. IL-7Rα expression on various immune compartments obtained from colonic LP of normal and colitic mice. *A*, Dot plot analysis shows the IL-7α expression on each fraction of immune cells from colonic LP of normal and colitic mice. Numerical values on the dot plots and histograms express the mean percentage of each fraction. *B*, The bar graphs show the MFI of IL-7Rα on each immune compartment obtained from colonic LP of normal and colitic mice. The graph data are the mean ± SEM. *$p < 0.05$. N.S., not significant.

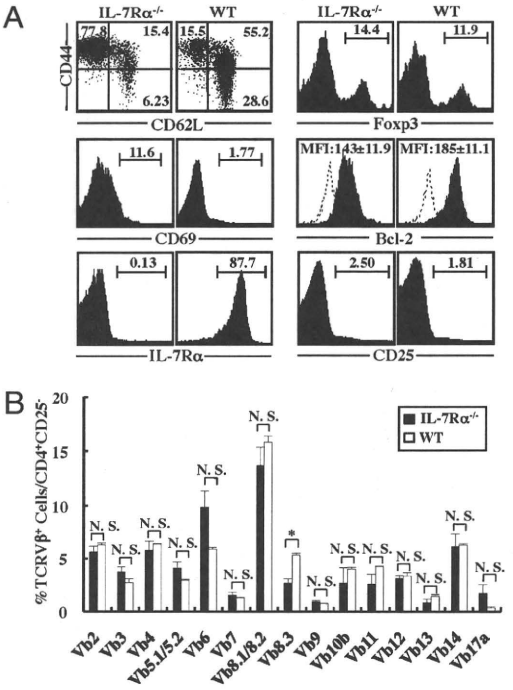

FIGURE 2. Phenotypic characterization of splenic CD4$^+$ T cells obtained from age-matched WT and IL-7Rα$^{-/-}$ mice. *A*, FACS analysis shows the expression of CD44/CD62L, IL-7Rα, Foxp3, and Bcl-2 on/in splenic CD4$^+$ T cells. The dotted line in the Bcl-2 histogram shows the baseline of isotype control. *B*, Flow cytometric analysis of Vβ families on the surface of the splenic CD4$^+$ T cells. To analyze the TCR Vβ family repertoire, splenic cells were double-stained with PE-conjugated anti-CD4 mAb (RM4-5) and a panel of 15 FITC-conjugated Vβ mAbs. The percentage value of each Vβ is the frequency pooled from three independent experiments ($n = 6$). The data are the mean ± SEM. *$p < 0.05$. N.S., not significant.

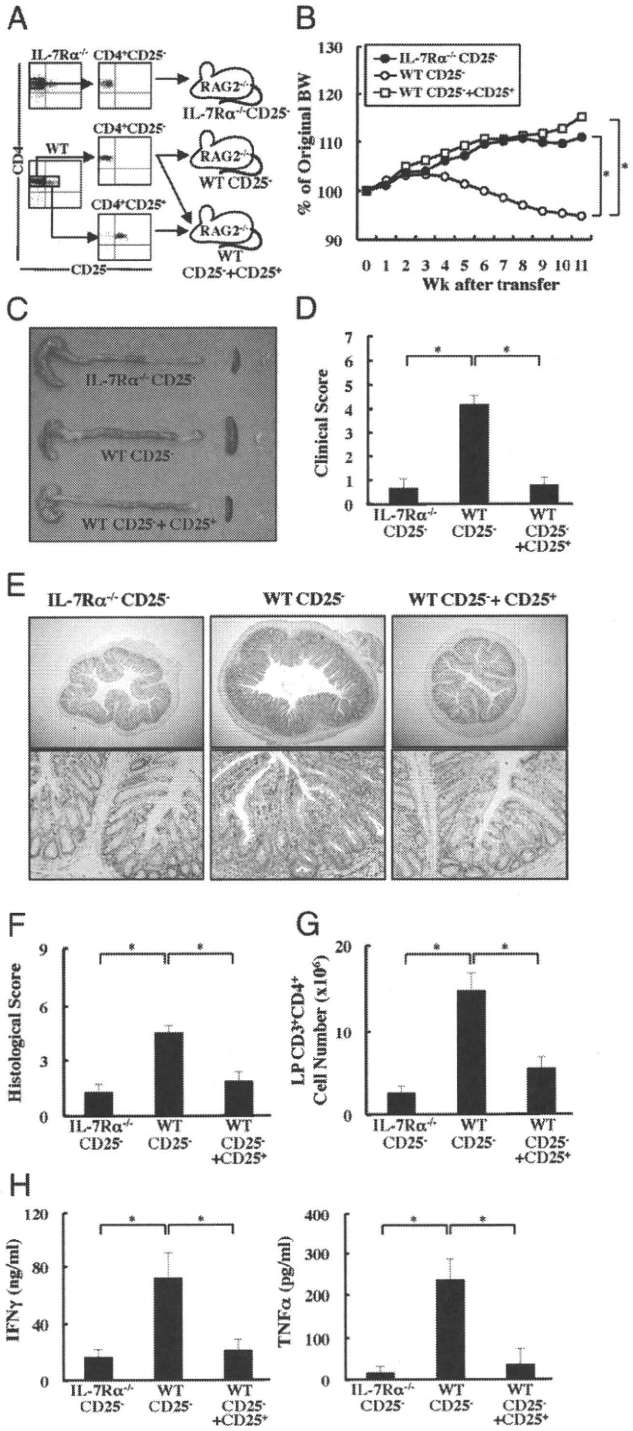

FIGURE 3. RAG-$2^{-/-}$ transferred with IL-7R$\alpha^{-/-}$ $CD4^+CD25^-$ T cells did not develop chronic colitis. *A*, RAG-$2^{-/-}$ mice were transferred with splenic $CD4^+CD25^-$ T cells obtained from age-matched WT or IL-7R$\alpha^{-/-}$ mice (3×10^5 cells per mouse). As a negative control, RAG-$2^{-/-}$ mice were transferred with splenic WT $CD4^+CD45RB^{high}$ T cells (3×10^5 cells per mouse) and $CD4^+CD25^+$ Tregs (1×10^5 cells per mouse). *B*, Change in body weight over time is expressed as a percentage of the original weight. Data are represented as the mean ± SEM of nine mice in each group. *$p < 0.05$, compared with colitic RAG-$2^{-/-}$ mice transferred with $CD4^+CD25^-$ T cells. *C*, Gross appearance of the colon, SP, and mesenteric lymph nodes from RAG-$2^{-/-}$ mice transferred with IL-7R$\alpha^{-/-}$ $CD4^+CD25^-$ T cells (*top*), RAG-$2^{-/-}$ mice transferred with WT $CD4^+CD25^-$ T cells (*middle*), and RAG-$1^{-/-}$ transferred with WT $CD4^+CD25^-$ T cells and $CD4^+CD25^+$ Tregs (*bottom*). *D*, Clinical scores were determined at 8 wk after the transfer as described in *Materials and Methods*. Data are indicated as the mean ± SEM of seven mice in each group. *$p < 0.001$. *E*, Histologic examination of the colon from RAG-$2^{-/-}$ mice transferred with IL-7R$\alpha^{-/-}$ $CD4^+CD25^-$ T cells (*left*), RAG-$2^{-/-}$ mice transferred with WT $CD4^+CD25^-$ T cells (*middle*), and RAG-$1^{-/-}$ transferred with WT $CD4^+CD25^-$ T cells and $CD4^+CD25^+$ Tregs (*right*) at 11 wk after the transfer. Original magnification ×40 (*upper*) and ×100 (*lower*). *F*, Histologic scoring at 11 wk after transfer. Data are indicated as the mean ± SEM of seven mice in each group. *$p < 0.05$. *G*, LP $CD3^+CD4^+$ T cells were isolated at 11 wk after transfer, and the number was determined by flow cytometry. Data are indicated as the mean ± SEM of seven mice in each group. *$p < 0.05$. *H*, Cytokine production by LP $CD4^+$ T cells. LP $CD4^+$ T cells were isolated at 11 wk after transfer and stimulated with anti-CD3 and anti-CD28 mAbs for 48 h. IFN-γ and TNF-α concentrations in culture supernatants were measured by ELISA. Data are indicated as the mean ± SD of seven mice in each group. *$p < 0.05$.

As a negative control, RAG-$2^{-/-}$ mice were transferred with a mixture of SP $CD4^+CD25^-$ T cells and $CD4^+CD25^+$ Tregs obtained from WT mice. As depicted in Fig. 3*B*, RAG-$2^{-/-}$ mice transferred with WT $CD4^+CD25^-$ T cells manifested progressive weight loss from 4 wk after transfer (Fig. 3*B*). In contrast, RAG-$2^{-/-}$ mice transferred with IL-7R$\alpha^{-/-}$ $CD4^+CD25^-$ T cells as well as RAG-$2^{-/-}$ mice transferred with a mixture of $CD4^+CD25^-$ T cells and $CD4^+CD25^+$ Tregs appeared healthy and showed a gradual increase of body weight (Fig. 3*B*). To check the possibility that mice transferred with IL-7R$\alpha^{-/-}$ $CD4^+CD25^-$ T cells develop colitis with delayed kinetics, we observed all groups of mice until 11 wk after transfer. Eleven weeks after transfer, RAG-$2^{-/-}$ mice transferred with WT $CD4^+CD25^-$ T cells, but not those transferred with IL-7R$\alpha^{-/-}$ $CD4^+CD25^-$ T cells or WT $CD4^+CD25^-$ T cells and $CD4^+CD25^+$ Tregs, had enlarged colons with greatly thickened walls (Fig. 3*C*). The same mice also showed the enlargement of SP and mesenteric lymph nodes (Fig. 3*C*). The assessment of colitis by clinical scores showed a clear difference between RAG-$2^{-/-}$ mice transferred with WT $CD4^+CD25^-$ T cells and the other two groups (Fig. 3*D*).

Histologic examination showed prominent epithelial hyperplasia with glandular elongation and massive infiltration of mononuclear cells in LP of RAG-$2^{-/-}$ mice transferred with WT $CD4^+CD25^-$ T cells (Fig. 3*E*, *middle panels*). In contrast, these inflammatory changes were mostly abrogated, and only a few mononuclear cells were observed in the LP of the colon from RAG-$2^{-/-}$ mice transferred with IL-7R$\alpha^{-/-}$ $CD4^+CD25^-$ T cells (Fig. 3*E*, *left panels*) or with a mixture of SP $CD4^+CD25^-$ T cells and $CD4^+CD25^+$ Tregs (Fig. 3*E*, *right panels*). This difference was also confirmed by the histologic scores of multiple colon sections: 5.35 ± 0.40 in RAG-$2^{-/-}$ mice transferred with WT $CD4^+CD25^-$ T cells versus 1.65 ± 0.57 in RAG-$2^{-/-}$ mice transferred with IL-7R$\alpha^{-/-}$ $CD4^+CD25^-$ T cells and 2.00 ± 0.74 in RAG-$2^{-/-}$ mice transferred with a mixture of SP $CD4^+CD25^-$ T cells and $CD4^+CD25^+$ Tregs ($p < 0.001$; Fig. 3*F*). Further quantitative evaluation of $CD4^+$ T cell infiltration was made by calculating the absolute cell number of LP $CD3^+CD4^+$ T cells recovered from the resected bowels. Significantly fewer $CD4^+$ T cells were recovered from the colonic tissue of RAG-$2^{-/-}$ mice transferred with IL-7R$\alpha^{-/-}$ $CD4^+CD25^-$ T cells or a mixture of SP $CD4^+CD25^-$ T cells and $CD4^+CD25^+$ Tregs as compared with colitic RAG-$2^{-/-}$ mice transferred with WT $CD4^+CD25^-$ T cells (Fig. 3*G*). We also examined the cytokine production by LP $CD4^+$ T cells. LP $CD4^+$ T cells from RAG-$2^{-/-}$ mice transferred with IL-7R$\alpha^{-/-}$ $CD4^+CD25^-$ T cells or a mixture of SP $CD4^+CD25^-$ T cells and $CD4^+CD25^+$ Tregs produced significantly lower amounts of IFN-γ and TNF-α than did colitic RAG-$2^{-/-}$ mice transferred with WT $CD4^+CD25^-$ T cells upon in vitro stimulation (Fig. 3*H*).

Importantly, further flow cytometric analysis revealed that almost all the SP and LP $CD3^+CD4^+$ T cells isolated from all three groups of mice at 11 wk after transfer were $CD44^{high}CD62L^-$ $CD69^+$ effector-memory T (T_{EM}) cells (Supplemental Fig. 1), indicating that the transferred $CD4^+CD25^-$ T cells could differentiate to activated T_{EM} cells regardless of the expression of IL-7Rα or the presence or absence of Tregs. These results suggest that the lack of IL-7Rα prevented the development of colitis primarily by inhibiting the expansion or survival of colitogenic $CD4^+$ T_{EM} cells in the colon in accordance with the lower expression of Bcl-2 (Fig. 2*A*). We found that SP and LP $CD4^+$ T cells isolated from all groups of mice at 11 wk after transfer did not express IL-15Rβ, which is a critical receptor for IL-15 signaling, and thymic stromal lymphopoietin (TSLP) receptor, which is critical for TSLP signaling via TSLPR/IL-7Rα complex receptors (Supplemental Fig. 1), indicating that IL-15 and TSLP may not be involved in this colitis model.

To further assess whether IL-7Rα$^{-/-}$ $CD4^+$ T cells are unable to produce inflammatory cytokines intrinsically or as the result of a secondary effect from disorder of cell proliferation or maintenance, we performed the following experiments. First, we accessed ex vivo cytokine production of IL-7Rα$^{-/-}$ or WT SP $CD4^+$ T cells under Th1 polarizing conditions (Supplemental Fig. 2*A*). As shown in Supplemental Fig. 2*B*, IL-7Rα$^{-/-}$ SP $CD4^+$ T cells expressed lower levels of IFN-γ than did WT SP $CD4^+$ T cells under the Th1 polarizing ex vivo conditions. This finding was confirmed by the statistical analysis (Supplemental Fig. 2*C*). Next, we examined the ability of the IL-7Rα$^{-/-}$ $CD4^+$ T cells to produce inflammatory cytokines under the same inflammatory conditions as the WT $CD4^+$ T cells. For this purpose, the same number (3×10^5 cells per mouse) of $Ly5.2^+$ IL-7Rα$^{-/-}$ SP $CD4^+$ $CD25^-$ T cells and $Ly5.1^+$ WT SP $CD4^+CD25^-$ T cells were cotransferred to RAG-2$^{-/-}$ recipients (Fig. 4*A*). The percentage of $Ly5.2^+$-derived IL-7Rα$^{-/-}$ T cells in peripheral blood was gradually decreased after transfer, while that of $Ly5.1^+$-derived WT T cells in peripheral blood was conversely increased, and the difference was significant 2 wk after transfer (Fig. 4*B*). Six weeks after transfer, all mice developed colitis (data not shown). Although the recovered cell number of $Ly5.2^+$ SP or LP $CD4^+$ T cells derived from IL-7Rα$^{-/-}$ donors at 6 wk after transfer was

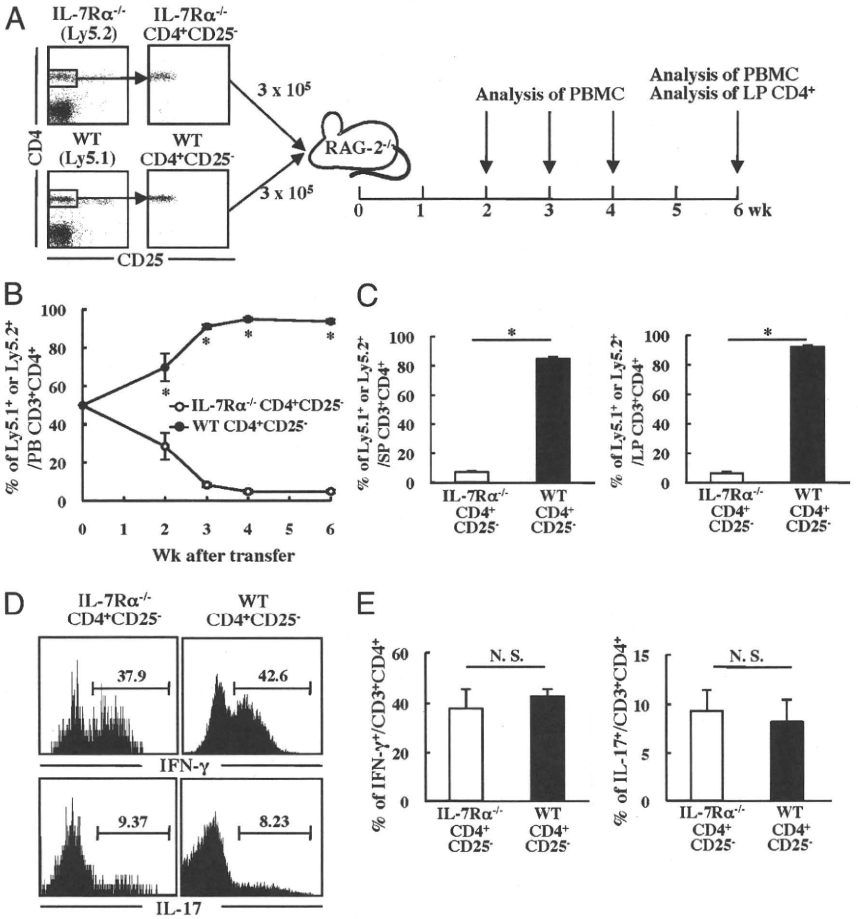

FIGURE 4. IL-7Rα$^{-/-}$ $CD4^+CD25^-$ T cells cotransferred with WT $CD4^+CD25^-$ T cells to RAG-2$^{-/-}$ mice could produce IFN-γ and IL-17, but could not survive. *A*, To discern why IL-7Rα$^{-/-}$ $CD4^+CD25^-$ T cells could not induce colitis, we cotransferred the same number (3×10^5) of $Ly5.2^+$ IL-7Rα$^{-/-}$ $CD4^+CD25^-$ T cells and $Ly5.1^+$ WT $CD4^+CD25^-$ T cells to $Ly5.2^+$ RAG-2$^{-/-}$ mice, and we compared the cell number and ability to produce Th1/Th17 cytokines between transferred IL-7Rα$^{-/-}$ and WT cells. PBMCs were collected 1, 2, 3, and 4 wk after the transfer. All mice were sacrificed and analyzed 6 wk after the transfer. *B*, Percentage of $Ly5.1^+$ or $Ly5.2^+$ cells in peripheral blood $CD3^+CD4^+$ cells at each time point were determined by flow cytometry. *C*, Percentage of $Ly5.1^+$ or $Ly5.2^+$ cells in SP and LP $CD3^+CD4^+$ cells 6 wk after the transfer. *D*, IFN-γ and IL-17 expression in recovered LP $CD4^+$ T cells from IL-7Rα$^{-/-}$ or WT donor mice. LP $CD4^+$ T cells were collected from RAG-2$^{-/-}$ recipients 6 wk after the transfer; they were cultured with ionomycin, PMA, and GolgiPlug for 12 h as mentioned in *Materials and Methods*. IFN-γ and IL-17 expression of them were determined by flow cytometry using intracellular staining methods. $CD3^+CD4^+Ly5.1^+$ cells were considered as $CD4^+$ T cells from WT donor mice, while $CD3^+CD4^+Ly5.1^-$ cells were considered as $CD4^+$ T cells from IL-7Rα$^{-/-}$ donor mice. Numerical values on the histograms express the mean percentage of each fraction. *E*, Percentage of IFN-γ^+ cells and IL-17^+ cells in LP $CD3^+CD4^+$ T cells from IL-7Rα$^{-/-}$ or WT donor mice. Data are indicated as the mean ± SEM of five mice in each group. $*p < 0.05$.

significantly lower than that from Ly5.1+ WT donors (Fig. 4*C*), both WT and IL-7Rα$^{-/-}$ donor-derived CD4+ T cells could similarly express IFN-γ and IL-17 in the colitic condition (Fig. 4*D*). These results indicate that IL-7Rα$^{-/-}$ cells in the absence of the neighboring WT cells cannot produce Th1 or Th17 cytokines as a result of suppression of colitis through a disorder of proliferation or maintenance, rather than intrinsically impaired ability.

As shown in Fig. 2*A*, the ratio of naive T cells in SP of IL-7Rα$^{-/-}$ mice was significantly lower than that of WT mice. Therefore, the possibility remains that this different ratio of naive-memory phenotypes of transferred cells might influence the strength of colitis. To rule out this possibility, we next performed another transfer experiment using the same number of naive CD4+ T cells (3×10^5 cells per mouse) as donor cells. RAG-2$^{-/-}$ mice were transferred with SP CD3+CD4+CD62L+CD44− naive T cells obtained from age-matched WT or IL-7Rα$^{-/-}$ mice (Fig. 5*A*). As a negative control, RAG-2$^{-/-}$ mice were transferred with SP WT naive T cells and CD4+CD25+ Tregs (Fig. 5*A*). As expected, neither mice transferred with IL-7Rα$^{-/-}$ naive T cells nor mice transferred with naive T cells and Tregs developed colitis as assessed by gross appearance of the colon (Fig. 5*B*), clinical (Fig. 5*C*) and histologic scorings (Fig. 5*D*, 5*E*), and the absolute cell number of LP CD3+CD4+ T cells (Fig. 5*F*) in sharp contrast to the diseased mice transferred with WT naive T cells, confirming that IL-7Rα expression on CD4+ T cells is essential for the development of colitis, regardless of the different ratio of naive and memory cells in SP of IL-7Rα$^{-/-}$ mice and WT mice. We further performed an apoptosis assay using annexin V/PI staining in this

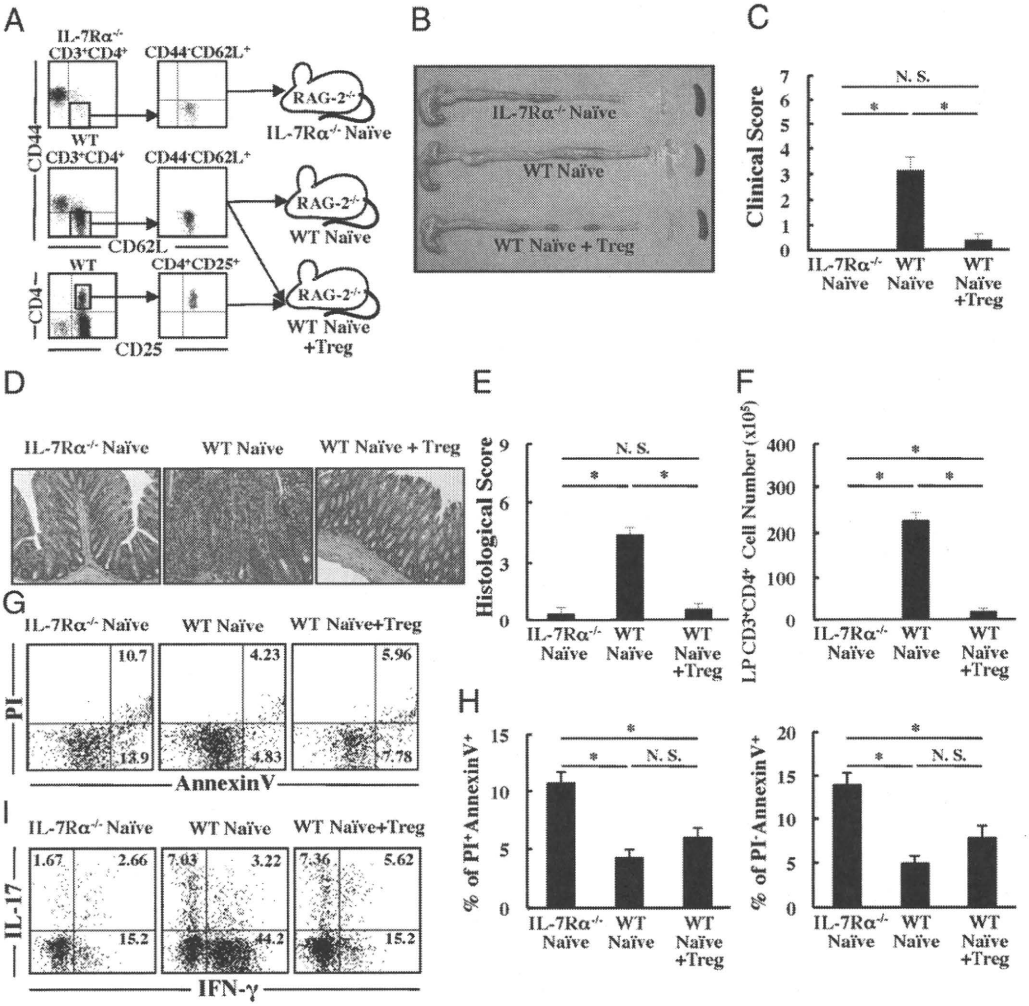

FIGURE 5. RAG-2$^{-/-}$ transferred with IL-7Rα$^{-/-}$ CD3+CD4+CD62L+CD44− T cells did not develop chronic colitis. *A*, RAG-2$^{-/-}$ mice were transferred with splenic CD3+CD4+CD62L+CD44− T cells obtained from age-matched WT or IL-7Rα$^{-/-}$ mice (3×10^5 cells per mouse). As a negative control, RAG-2$^{-/-}$ mice were transferred with splenic WT CD3+CD4+CD62L+CD44− T cells (3×10^5 cells per mouse) and CD4+CD25+ Tregs (1×10^5 cells per mouse). *B*, Gross appearance of the colon, SP, and mesenteric lymph nodes from RAG-2$^{-/-}$ mice transferred with IL-7Rα$^{-/-}$ CD3+CD4+CD62L+CD44− (*top*), RAG-2$^{-/-}$ mice transferred with WT CD3+CD4+CD62L+CD44− T cells (*middle*), and RAG-1$^{-/-}$ transferred with WT CD3+CD4+CD62L+CD44− T cells and CD4+CD25+ Tregs (*bottom*). *C*, Clinical scores were determined at 8 wk after the transfer as described in *Materials and Methods*. Data are indicated as the mean ± SEM of each group. *$p < 0.05$. *D*, Histologic examination of the colon from RAG-2$^{-/-}$ mice transferred with IL-7Rα$^{-/-}$ CD3+CD4+CD62L+CD44− T cells (*left*), RAG-2$^{-/-}$ mice transferred with WT CD3+CD4+CD62L+CD44− T cells (*middle*), and RAG-1$^{-/-}$ transferred with WT CD3+CD4+CD62L+CD44− T cells and CD4+CD25+ Tregs (*right*) at 8 wk after the transfer. Original magnification ×40 (*upper*) and ×100 (*lower*). *E*, Histologic scoring at 8 wk after transfer. Data are indicated as the mean ± SEM of each group. *$p < 0.05$. *F*, LP CD3+CD4+ T cells were isolated at 8 wk after transfer, and the number was determined by flow cytometry. Data are indicated as the mean ± SEM of each group. *$p < 0.05$. *G*, The expression of propidium iodide (PI) and annexin V in SP CD4+ T cells from RAG-2$^{-/-}$ mice transferred with IL-7Rα$^{-/-}$ CD3+CD4+CD62L+CD44− T cells, RAG-2$^{-/-}$ mice transferred with WT CD3+CD4+CD62L+CD44− T cells, and RAG-2$^{-/-}$ transferred with WT CD3+CD4+CD62L+CD44− T cells and CD4+CD25+ Tregs at 8 wk after the transfer. *H*, The percentage of early apoptotic cells (annexin V+PI−) and late apoptotic cells (annexin V+PI−). *I*, Intracellular staining of cytokines (IL-17/IFN-γ) in the colonic LP CD4+ T cells. Numerical values on the dot plots and histograms express the mean percentage of each fraction.

setting. IL-7Rα$^{-/-}$ SP CD4$^+$ T cells underwent apoptosis more frequently than WT SP CD4$^+$ T cells (Fig. 5*G*, 5*H*), which supports the hypothesis that expression of IL-7Rα on CD4$^+$ T cells is important for their survival. Furthermore, the expression of IL-17 and IFN-γ in IL-7Rα$^{-/-}$ LP CD4$^+$ T cells was markedly decreased compared with that in WT LP CD4$^+$ T cells (Fig. 5*I*).

IL-7Rα$^{-/-}$ × RAG-2$^{-/-}$ mice transferred with CD4$^+$CD25$^-$ T cells developed colitis

To further assess the role of IL-7/IL-7R signaling in the development of chronic colitis, we next focused on IL-7Rα expression on non-T cells, such as APCs and NK cells that reside in RAG-2$^{-/-}$ recipients, because it is possible that IL-7 is competitively used by various IL-7Rα–expressing immune compartments, and the competition may affect the development of chronic colitis. To test this hypothesis, WT CD4$^+$CD25$^-$ T cells were transferred into RAG-2$^{-/-}$ or IL-7Rα$^{-/-}$ × RAG-2$^{-/-}$ mice (Fig. 6*A*). As a negative control, a mixture of WT CD4$^+$CD25$^-$ T cells and CD4$^+$CD25$^+$ Tregs was transferred into RAG-2$^{-/-}$ mice (Fig. 6*A*). When CD4$^+$CD25$^-$ T cells were transferred into the control RAG-2$^{-/-}$ mice, the recipients, as expected, rapidly developed severe wasting disease associated with clinical signs of severe colitis, in particular, weight loss, persistent diarrhea and occasionally bloody stool and anal prolapses, in sharp contrast to healthy RAG-2$^{-/-}$ mice transferred with a mixture of CD4$^+$ CD25$^-$ T cells and CD4$^+$CD25$^+$ Tregs (Fig. 6*B*). When CD4$^+$ CD25$^-$ T cells were transferred into the IL-7Rα$^{-/-}$ × RAG-2$^{-/-}$ mice, the recipients also developed severe wasting chronic colitis (Fig. 6*B*). These RAG-2$^{-/-}$ and IL-7Rα$^{-/-}$ × RAG-2$^{-/-}$ mice transferred with CD4$^+$CD25$^-$ T cells, but not RAG-2$^{-/-}$ mice transferred with a mixture of CD4$^+$CD25$^-$ T cells and CD4$^+$ CD25$^+$ Tregs, had enlarged colons with significantly thickened walls accompanied with enlarged SPs and mesenteric lymph nodes 8 wk after transfer (Fig. 6*C*). Consistent with this finding, clinical scores of RAG-2$^{-/-}$ and IL-7Rα$^{-/-}$ × RAG-2$^{-/-}$ mice transferred with CD4$^+$CD25$^-$ T cells were significantly higher than those of RAG-2$^{-/-}$ mice transferred with a mixture of CD4$^+$ CD25$^-$ T cells and CD4$^+$CD25$^+$ Tregs (Fig. 6*D*). No significant difference in clinical scores was found between RAG-2$^{-/-}$ and IL-7Rα$^{-/-}$ × RAG-2$^{-/-}$ mice transferred with CD4$^+$CD25$^-$ T cells, although the score of IL-7Rα$^{-/-}$ × RAG-2$^{-/-}$ mice tended to be higher than that of RAG-2$^{-/-}$ mice transferred with CD4$^+$CD25$^-$ T cells (Fig. 6*D*).

Histologic examination showed that tissue sections from RAG-2$^{-/-}$ and IL-7Rα$^{-/-}$ × RAG-2$^{-/-}$ mice transferred with CD4$^+$ CD25$^-$ T cells were characterized by inflammatory infiltrate, epithelial hyperplasia, crypt cell damage, and goblet cell depletion, in contrast to RAG-2$^{-/-}$ mice transferred with a mixture of CD4$^+$CD25$^-$ T cells and CD4$^+$CD25$^+$ Tregs, which showed no features of colitis (Fig. 6*E*). This difference was also confirmed by histologic scoring of multiple colon sections (Fig. 6*F*). Consistent with the histologic assessment, the numbers of LP CD4$^+$ T cells recovered from RAG-2$^{-/-}$ and IL-7Rα$^{-/-}$ × RAG-2$^{-/-}$ mice transferred with CD4$^+$CD25$^-$ T cells were similar to each other but significantly higher than that from noncolitic RAG-2$^{-/-}$ mice transferred with a mixture of CD4$^+$CD25$^-$ T cells and CD4$^+$ CD25$^+$ Tregs (Fig. 6*G*). Cytokine production by LP CD4$^+$ T cells is depicted in Fig. 6*H*. LP CD4$^+$ T cells from RAG-2$^{-/-}$ and IL-7Rα$^{-/-}$ × RAG-2$^{-/-}$ mice transferred with CD4$^+$CD25$^-$ T cells produced significantly higher levels of IFN-γ and TNF-α than did those from the control mice transferred with a mixture of CD4$^+$ CD25$^-$ T cells and CD4$^+$CD25$^+$ Tregs (Fig. 6*H*).

Flow cytometric analysis revealed that the LP CD4$^+$ T cells isolated from all groups of mice at 8 wk after transfer were CD44^{high}CD62L$^-$CD69$^+$ T_{EM} cells (Supplemental Fig. 3*A*), indicating that the transferred CD4$^+$CD25$^-$ T cells could differentiate to activated T_{EM} cells regardless of the presence or absence of IL-7Rα on non-T cells in the RAG-2$^{-/-}$ recipient mice. Intracellular analysis further showed that almost the same fraction of LP CD4$^+$ T cells from both RAG-2$^{-/-}$ and IL-7Rα$^{-/-}$ × RAG-2$^{-/-}$ mice transferred with CD4$^+$CD25$^-$ T cells had differentiated to IFN-γ–producing Th1 or IL-17–producing Th17 (Supplemental Fig. 3*B*). In contrast, the expression of IFN-γ in LP CD4$^+$ T cells from RAG-2$^{-/-}$ mice transferred with a mixture of CD4$^+$CD25$^+$ and CD4$^+$CD25$^-$ T cells was markedly reduced as compared with the groups with colitis (Supplemental Fig. 3*B*).

To further clarify whether the lower number of CD4$^+$CD25$^-$ T cells in the transfer experiment makes this difference significant, RAG-2$^{-/-}$ mice and IL-7Rα$^{-/-}$ × RAG-2$^{-/-}$ mice were transferred with 3×10^5 or 1×10^5 WT SP CD4$^+$CD25$^-$ T cells. As a negative control, RAG-2$^{-/-}$ mice were transferred with splenic WT CD4$^+$CD25$^-$ T cells (3×10^5 cells per mouse) and CD4$^+$ CD25$^+$ Tregs (3×10^5 cells per mouse; Supplemental Fig. 4*A*). However, no differences were found in clinical and histologic colitis scores or the absolute number of LP CD3$^+$CD4$^+$ T cells between IL-7Rα$^{-/-}$ and WT transferred groups, irrespective of lower or higher number of donor T cells (Supplemental Fig. 4*B*–*E*). Although we also checked the expression of MHC class II on CD11b$^-$CD11c$^+$ classical dendritic cells and CD11b$^+$CD11c$^+$ myeloid dendritic cells in this experiment (Supplemental Fig. 4*F*), no differences were detected between any groups. Diminished expression of MHC class II on dendritic cells in RAG-2$^{-/-}$ mice, which is caused by elevated level of IL-7 with lymphopenia, may recover after transferred CD4$^+$ T cells consume IL-7.

Discussion

This study has demonstrated that the high expression of IL-7Rα on colitic CD4$^+$ T cells, but not on non-T cells, is essential for the development and persistence of colitis. This finding is supported by the findings that 1) the MFI of IL-7Rα expression of LP CD4$^+$ T cells is significantly higher than that of other non-CD4$^+$ T cells in colitic conditions, 2) the MFI of IL-7Rα expression of colitic LP CD4$^+$ T cells is significantly higher than that of normal LP CD4$^+$ T cells, 3) RAG-2$^{-/-}$ mice transferred with IL-7Rα$^{-/-}$ CD4$^+$CD25$^-$ T cells do not develop colitis, and 4) IL-7Rα$^{-/-}$ × RAG-2$^{-/-}$ mice transferred with WT CD4$^+$CD25$^-$ T cells develop colitis similar to that in transferred IL-7Rα$^{+/+}$ × RAG-2$^{-/-}$ mice. Collectively, IL-7Rα expression on colitic CD4$^+$ T, but not on other cells, is essential for the development and persistence of chronic colitis.

It was originally reported that IL-7Rα is highly expressed on lymphocytes such as T cells (16). Consistent with this report, we have previously reported that the IL-7/IL-7R signaling pathway is critical for the maintenance of IL-7Rα^{high} colitogenic CD4$^+$ memory T cells (18, 20). Furthermore, we showed that treatment with neutralizing anti–IL-7Rα mAb ameliorated ongoing chronic colitis (18). More recently, several reports have proved the importance of the IL-7/IL-7R signal in nonlymphocytes. Guimond et al. (31) have reported that IL-7Rα is expressed on some types of dendritic cells, and that in the lymphopenic environment the IL-7/IL-7R signal of dendritic cells leads to depression of its MHC class II molecule, which results in the suppression of the proliferation of CD4$^+$ T cells. Other recent reports that IL-7Rα is broadly expressed on NK cells, dendritic cells, and macrophages in normal conditions (16, 17), suggesting the need for us to further investigate the importance of the IL-7/IL-7R signaling pathway in non-T cells for the development and persistence of chronic colitis. Although IL-7Rα expression on